

1964

# Tests on A36 and A441 steel beam-columns

Richard A. Aglietti  
*Lehigh University*

Follow this and additional works at: <https://preserve.lehigh.edu/etd>



Part of the [Civil Engineering Commons](#)

---

## Recommended Citation

Aglietti, Richard A., "Tests on A36 and A441 steel beam-columns" (1964). *Theses and Dissertations*. 3180.  
<https://preserve.lehigh.edu/etd/3180>

This Thesis is brought to you for free and open access by Lehigh Preserve. It has been accepted for inclusion in Theses and Dissertations by an authorized administrator of Lehigh Preserve. For more information, please contact [preserve@lehigh.edu](mailto:preserve@lehigh.edu).

TESTS ON A36 AND A441 STEEL  
BEAM-COLUMNS

by  
Richard A. Aglietti

A THESIS  
Presented to the Graduate Faculty  
of Lehigh University  
in Candidacy for the Degree of  
Master of Science

Lehigh University

1964

## A B S T R A C T

This thesis describes an experimental study of five rolled 8WF31 steel beam-columns which was performed in order to determine their strength and deformation behavior. The beam-column ends are essentially fixed about their weak axis and pinned about their strong axis. Warping of the end section is fully restrained by end plates. End moments are applied in the plane of the web in order to cause bending about the strong axis and the end moments can be varied independently of the axial load.

Two of the beam-columns were rolled from ASTM-A441 steel and three were rolled from ASTM-A36 steel. The principal test variables are the axial load, the slenderness ratio, the grade of steel, the absence or presence of lateral bracing, and the absence or presence of restraining beams. The purposes of the investigation are:

- a) to test the effect of a lateral-torsional buckling on the behavior of beam-columns under relatively high axial loads
- b) to check a theory developed for A7 steel on members of A441 steel

The testing program, the test setup, and procedures used during testing are described. The effects of axial load and lateral bracing are discussed. The results are then compared with "in-plane" bending theory and inelastic lateral-torsional buckling theory. Finally the experimental results are compared with a commonly used empirical interaction equation.

C E R T I F I C A T E O F A P P R O V A L

This thesis is accepted and approved in partial fulfillment  
of the requirements for the degree of Master of Science in  
Civil Engineering.

May 19, 1964

(Date)

T. V. Galambos  
Professor Theodore V. Galambos  
Professor in Charge

W. J. Eney  
Professor William J. Eney, Head  
Department of Civil Engineering

A C K N O W L E D G M E N T S

The author is indebted to Dr. Theodore V. Galambos, Professor in charge of the thesis, for his criticisms and guidance during its preparation. He also wishes to express special thanks to Mr. Maxwell G. Lay for his very helpful advice.

The work contained in this thesis is part of an investigation on "Welded Continuous Frames and Their Components" being conducted under the direction of Dr. George C. Driscoll, Jr.. Dr. Lynn S. Beedle is director of Fritz Engineering Laboratory where the work was performed and Professor William J. Eney is head of the Laboratory and Civil Engineering Department. The project is sponsored jointly by the Welding Research Council and the Department of the Navy. Funds are furnished by the American Institute of Steel Construction, American Iron and Steel Institute, Institute of Research at Lehigh University, Office of Naval Research, Bureau of Ships, and the Bureau of Yards and Docks. The Column Research Council acts in an advisory capacity.

The assistance of Mr. Peter Adams, Mr. Balmukund Parikh, Mr. Robert Dales and the laboratory technicians in making the test setups and helping to run the tests is gratefully acknowledged. The thesis was typed by Miss Gloria Teles and the drawings were prepared by Mr. Ronald Weiss. Their help is greatly appreciated.

TABLE OF CONTENTS

	Page
SYNOPSIS	1
1. INTRODUCTION	2
1.1 Purpose of the Experiments	2
1.2 Comparison with Other Column Experiments	3
2. DESCRIPTION OF THE EXPERIMENTS	5
2.1 Test Program	5
(a) Material	6
(b) Load Application	7
2.2 Experimental Apparatus and Procedures	7
3. DISCUSSION OF THE TEST RESULTS	11
3.1 Test Results	11
3.2 Influence of Axial Force	14
3.3 Influence of Lateral-Torsional Buckling	15
4. COMPARISON OF THE TEST RESULTS WITH INELASTIC THEORY	16
4.1 Comparison with Inelastic Lateral-Torsional Buckling Theory	16
4.2 Comparison with Bending Theory	20
5. COMPARISON OF THE TEST RESULTS WITH THE CRC INTERACTION EQUATION	22
6. SUMMARY AND CONCLUSIONS	24
7. NOMENCLATURE	26
8. TABLES AND FIGURES	28
9. REFERENCES	57
10. VITA	59

v

LIST OF TABLES

<u>Table</u>		<u>Page</u>
1.	Testing Program	29
2.	Measured Cross Section Properties	30
3.	Material and Length Properties	31
4.	Experimental Results	32
5.	Comparison of Experiments with Theory	33

LIST OF FIGURES

<u>Figure No.</u>		<u>Page</u>
1	Front View of a Typical Test Setup	34
2	Rear View of a Typical Test Setup	35
3	Connection and End Fixture	36
4	Test Subassemblage (RC-3 and RC-10)	37
5	Restrained Column End Detail	38
6	Joint Moments	39
7	Braced Joint	40
8	Excessive Bending and Lateral-Torsional Buckling Behavior	41
9	Test HT-39 Experimental Results	42
10	Test HT-40 Experimental Results	43
11	Test RC-8 Experimental Results	44
12	Test RC-9 Experimental Results	45
13	Test RC-10 Experimental Results	46
14	Moment-Twist Curves	47
15	RC-8 and RC-9 Comparison Curves	48
16	HT-39 and HT-40 Comparison Curves	49
17	RC-3 and RC-10 Comparison Curves	50
18	Upper Bound and Lower Bound Moment Diagrams	51
19	Upper and Lower Bound Flow Sheet	52



<u>Figure No.</u>		<u>Page</u>
20	Comparison of HT-40 with Theory	53
21	Comparison of RC-8 with Theory	54
22	Comparison of RC-9 with Theory	55
23	Comparison of RC-10 with Theory	56
24	Comparison of Tests with the CRC Interaction Equation	57

S Y N O P S I S

This thesis describes an experimental study of five rolled 8WF31 steel beam-columns which was performed in order to determine their strength and deformation behavior. The beam-column ends are essentially fixed about their weak axis and pinned about their strong axis. Warping of the end section is fully restrained by end plates. End moments are applied in the plane of the web in order to cause bending about the strong axis and the end moments can be varied independently of the axial load.

Two of the beam-columns were rolled from ASTM-A441 steel and three were rolled from ASTM-A36 steel. The principal test variables are the axial load, the slenderness ratio, the grade of steel, the absence or presence of lateral bracing, and the absence or presence of restraining beams. The purposes of the investigation are:

- a) to test the effect of a lateral-torsional buckling on the behavior of beam-columns under relatively high axial loads
- b) to check a theory developed for A7 steel on members of A441 steel

The testing program, the test setup, and procedures used during testing are described. The effects of axial load and lateral bracing are discussed. The results are then compared with "in-plane" bending theory and inelastic lateral-torsional buckling theory. Finally the experimental results are compared with a commonly used empirical interaction equation.

## 1. INTRODUCTION

### 1.1 PURPOSE OF THE EXPERIMENTS

In plastic theory, a structure is said to have failed when it is loaded with the maximum load which the structure as a whole can support and not as the attainment of the load corresponding to the maximum strength of one of its individual members. Theoretical methods of analysis have been developed wherein the beam-column is considered as an integral part of a structural subassembly rather than an isolated member. (1) (2) (3) The development of column design based on the ultimate strength of such a subassembly presupposes a knowledge of the end moment-end rotation behavior of the unrestrained beam-column. (2) References 4 and 5 present two different approaches to the solution of this type of problem, but in either case it is assumed that the beam-column will fail by excessive bending about one of its principal axes. Thus, if the end moments of a beam-column act in the plane of the web, adequate bracing must be provided to prevent the occurrence of lateral-torsional buckling. It is further assumed in these two references that the material from which the beam-column is made is ASTM-A7 steel. However, adjustment may be made in order to take into account the difference in yield strength which exists in different grades of steel.

In an actual structure, a beam-column which is braced adequately to prevent lateral-torsional buckling may not always be feasible and furthermore the increasing use of high strength steels demands a more refined knowledge of the responses of members composed of these steels when under load. It is for these two reasons that the five beam-column experiments which are described in this report were conducted.

In this investigation four pinned-end beam-columns and one restrained beam-column were tested. Sidesway of the top of the member with respect to its bottom, and biaxial bending, were not intentionally introduced. The beam-columns were defined by the following parameters: axial load, slenderness ratio, absence or presence of lateral bracing, grade of steel, and the absence or presence of restraining beams. The test specimens were subjected to equal end moments causing single curvature deformations about their strong axis.

## 1.2 COMPARISON WITH OTHER COLUMN EXPERIMENTS

Van Kuren and Galambos<sup>(6)</sup> present a brief description of major beam-column experiments reported in the literature and describe 42 additional beam-column experiments on wide-flange beam-columns subjected to axial force and bending moments about the strong axis conducted at Lehigh University. The effects of axial force, length, member size, lateral bracing, and loading conditions were studied. Eight of these tests were loaded similarly to those discussed here, that is axial load plus equal end moments causing single curvature bending about the strong axis.

The beam-column experiments described here differ from those which have been previously reported in the following points:

- (a) The determination of the effect of lateral-torsional buckling on the strength of beam-columns under considerably higher axial loads was a primary objective.
- (b) Two of the specimens were made of high strength steel (ASTM-A441).
- (c) One of the specimens was a restrained, unbraced beam-column.

The objectives of the experiments were to check on an available lateral-torsional buckling theory, to check "in-plane" behavior and buckling behavior of high strength steel beam-columns as part of an investigation directed toward the extension of plastic design theories to high strength steel, and, finally, to compare the behavior of an unbraced restrained beam-column with an identical specimen, the latter being braced to prevent the occurrence of lateral-torsional buckling. (7)

## 2. DESCRIPTION OF THE EXPERIMENTS

The testing program in general has been briefly described in the introduction. In this section the test variables will be discussed, and the experimental procedures and the apparatus used will be described.

### 2.1 TEST PROGRAM

Table 1 outlines the testing program. Each of the five tests is listed with its principal variables. Test RC-3 was not included in this particular series of tests but it is included in this table for comparison purposes with test RC-10. The principal variables investigated are the axial load ratio  $P/P_y$ , the strong axis slenderness ratio  $L/r_x$ , and the effect of lateral bracing. Two of the tests were on beam-columns of high strength steel. At present, no comparison can be made between these two tests and tests performed on beam-columns made of lower strength steel because no previous test could be found wherein the grade of steel was the only variable.

The values of  $P/P_y$  and  $L/r_x$  given in Table 1 are nominal values. Table 4 gives the exact experimental values. The measured cross sectional properties (that is, area  $A$ , strong axis section modulus  $S_x$ , strong axis plastic modulus  $Z_x$ , and the major and minor radii of gyration,  $r_x$  and  $r_y$ ) are presented in Table 2. The static yield stress  $\sigma_y$ , the yield load  $P_y$  ( $A\sigma_y$ ), the yield moment  $M_y$  ( $S_x\sigma_y$ ), the plastic moment  $M_p$  ( $Z_x\sigma_y$ ), the length and the true slenderness ratio are given in Table 3. Finally, Table 4 summarizes the experimental

results by listing the experimental axial load  $P$ , the maximum end moment  $M_o$ , and the non-dimensionalized maximum end moment  $M_o/M_p$ . These four tables present the essential results of the test program.

(a) Material

The beam-columns for tests HT-39 and HT-40 were rolled from ASTM-A441 steel. The specimens for the remaining three tests (designated as RC-8, RC-9, and RC-10) were rolled from ASTM-A36 steel. The beam-columns were tested in an "as-delivered" condition, thus residual stresses were present. The magnitude and distribution of the rolling residual stresses were determined for the beam-column section (8WF31) of A441 steel from a length from the same heat. The distributions were close to the standard pattern and the values obtained were no greater than that for A7 steel. The maximum measured compressive residual stress was  $0.27\sigma_y$ . The residual stresses for the A36 beam-columns were similarly determined and the maximum compressive residual stress was found to be  $0.52\sigma_y$ . The average of the four flange tips was  $0.27\sigma_y^{(8)}$ .

The yield stress was determined for each specimen by testing standard tension coupons cut from an unyielded portion of the "tension" flange of the tested beam-column. These values (as listed in Table 3) do not include the effect of strain rate (they are "static" values).

(b) Load Application

For all five tests a predetermined axial load was applied first to the beam-column. This axial load was then decreased while end bending moments were applied by hydraulic jack through a lever arm so that the sum of the axial load produced by the testing machine and the jack force was always constant.<sup>(7)</sup> The beam-column was said to have reached ultimate strength when it resisted the maximum end bending moment that it was capable of resisting.

In the first two tests (HT tests), one of the specimens was braced. Bracing was provided at the mid-height and at points 5 ft. on either side of the mid-height. The unbraced length was within the span required in order to prevent lateral-torsional buckling.<sup>(9)</sup> In the second test no intermediate lateral bracing was used and as a result, it failed by lateral-torsional buckling. In the remaining three tests (RC tests) none of the beam-columns were braced and again failure occurred by lateral-torsional buckling. Test RC-3 was braced at the mid-height and 4 ft. 6 in. on either side of the mid-height.<sup>(9)</sup> The bracing proved adequate and failure occurred by excessive bending in the plane of the applied moments.

2.2 EXPERIMENTAL APPARATUS AND PROCEDURES

The front view of a general test set-up is shown in Figure 1. The two end fixtures which provided a pinned condition about the strong axis and an essentially fixed condition about the weak axis are shown and the



rotation bars which were used to measure the end rotations can be seen. Figure 2 is a rear view of a general test set-up. The hydraulic jack which introduced the applied moments and the dynamometer which measured the jack force can be seen and the dial gage arrangements used to measure mid-height transverse and lateral deflections are shown. The apparatus described in Reference 7 was used. Since it has already been described in detail only the modifications as they apply to this series of tests will be discussed.

Tests HT-39, HT-40, RC-8, and RC-9 were tested as pinned end beam-columns, that is, the restraining beams described in Reference 7 were omitted. Test HT-39 was a braced specimen<sup>(7)</sup> and the remaining three beam-columns were tested without the bracing. Figure 3 shows an end connection and end fixture detail for an isolated beam-column test. The end fixtures shown diagrammatically, ensure that the axial load will always pass through two fixed points, one at each end of the specimen. The points are the centers of the cylindrical surfaces (Point 0 in Figure 3) and the test beam-columns are designed in order that the centers of the cylindrical surfaces are also the centers of the joint details.

The beam-column in test RC-10 was a restrained column identical to test RC-3<sup>(7)</sup> <sup>(8)</sup> with the exception that it was not braced. Figure 4 diagrammatically shows the test layout. The restraining beams were 5WF 18.5 sections and they were 8 ft. long. The design of the subassemblage test member and its validity in checking frame theory<sup>(3)</sup> are also discussed in Reference 7.

Tests HT-39 and RC-3 (braced specimens) failed by excessive bending in the plane of the applied moments and tests HT-40, RC-8, RC-9, and RC-10 (unbraced specimens) failed by lateral-torsional buckling.

A photograph of the end connection and fixture for a restrained column test is given in Figure 5. The entire moment produced by the jack working over a lever arm is no longer resisted by only the column. Conditions of equilibrium and compatibility require that the restraining beam also resist the applied moment. Figure 6 shows that the applied moment,  $M_j$  is resisted by the column end moment,  $M_{c(j)}$  and the beam moment,  $M_B$ . Therefore, as shown in Figure 7, for any amount of joint rotation, the column end moment, A and the restraining beam end moment, B must be added together to obtain the joint moment, (A+B).

The length and size of the restraining beams determines the amount of restraint produced, and thus the effect on the moment-rotation behavior of the subassembly.<sup>(7)</sup> Tests RC-3 and RC-10 had relatively short restraining beams (8 feet). In each case a plastic hinge formed in the beams before the maximum capacity of the joint was reached. Unloading of the joint was precipitated by unloading of the column.<sup>(7)</sup>

The function of the bracing in tests HT-39 and RC-3 was to ensure against lateral-torsional buckling. Since lateral-torsional buckling was anticipated for the unbraced beam-columns, mid-height lateral deflection readings were taken by viewing a scale (graduated in 100ths) at three points (the two flange tips and the centerline of the web) through a transit. Two dial gages were mounted to the testing machine frame and

by means of a thin wire connection to the beam-column flange tips, mid-height lateral beam-column movements were again obtained.

All other deformations and forces were measured using the apparatus and techniques described in Reference 7. Strains were measured with SR-4 gages, transverse deflections were measured with dial gages connected to the beam-column with thin wire, and end rotations were measured by the level bar method.

In brief the test procedure for each test was as follows:

- a) The preliminary work consisted of the measurement of the beam-column dimensions, the predictions of the mode of failure, the calculation of the load expected at ultimate strength, and the preparation of the predicted moment-rotation curve.
- b) During the actual testing of the beam-column, after each increment of moment was applied, time was allowed for the system to come to rest before readings were taken. This was especially true after first yield. Strain rate effects were thus eliminated and the readings represented a static condition. In the inelastic range increments of rotation rather than increments of load were used.
- c) Loading was usually continued until the axial load which the beam-column supported could no longer be maintained. In all tests some unloading of the applied moment was observed.

### 3. DISCUSSION OF THE TEST RESULTS

A beam-column is defined here to have reached ultimate load when the maximum moment is reached and the beam-column starts to unload, that is the instant the maximum point on the moment-rotation curve is reached. In Figure 8 points F and D will be defined as the criterion for the ultimate strength for excessive bending behavior and lateral-torsional buckling behavior respectively.

Lateral-torsional buckling behavior is described by curve ABCDE. At point C the beam-column begins to twist and move laterally and at point D the ultimate moment is reached.

Curve ABCFG represents "in-plane" behavior of a beam-column. At point F, as defined above, ultimate strength is reached. This type of behavior can be expected for beam-columns bent about the strong axis only if adequate lateral bracing is provided.

#### 3.1 TEST RESULTS

The principal test results are the maximum bending moment which a beam-column can support in addition to its constant axial force, the end moment-versus-end slope curve, and observations of the type and cause of failure.

The load parameters may be found in Table 4. Test HT-39, the braced column failed by excessive bending in the plane of the applied moments and the four remaining tests, which were tested without bracing, failed by lateral-torsional buckling.

The moment-rotation curves represent the most important results of the experiments. A comparison will now be made between the experimental moment-rotation curves and the curves determined by "in-plane" theory<sup>(5)</sup> (10) (11). The experimental moment-rotation curves for each test are given in Figures 9 through 13.

The theoretical test curves were determined from the available column deflection curve data.<sup>(5)</sup> For specific values of end slope the corresponding end moments were determined and the end moment-versus-end slope curve was plotted. For the high strength steel tests (A441) the theoretical curves were based on a yield stress of 55 ksi and for the remaining three tests (A36) the theoretical curves were for 33 ksi steel.

Figure 9 shows the predicted and experimental curves for test HT-39. The theoretical curve assumes a yield stress of 55 ksi and  $P = 0.4P_y$ . Since the beam-column was adequately braced it was expected that the maximum end moment would approximately reach the predicted  $M_o/M_p = 0.236$ . It was able to attain a value of  $M_o/M_p = 0.228$ , 3.39% below the prediction. The difference in the elastic slopes of the two curves is explained by the fact that the test axial load ratio was  $P/P_y = 0.425$  rather than the anticipated  $P/P_y = 0.400$ .

The theoretical curve in Figure 10 is a prediction of the "in-plane" behavior of beam-column HT-40. Since the specimen was unbraced, it was expected that lateral-torsional buckling would occur before the attainment of the "in-plane" maximum moment. This was what actually occurred. The load dropped off very sharply because the specimen twisted into an unstable configuration. The result was that the beam-column had

a very small rotation capacity. The specimen managed to reach a value of  $M_o/M_p = 0.208$ , only 7.56% below the "in-plane" ultimate moment.

Tension coupons cut from the already tested specimens of tests RC-8 and RC-9 showed that the static yield stress had a value of 33.6 ksi. As a result, the test curves for these two tests are shown in comparison with curves drawn assuming a yield stress value of 33 ksi (Figures 11 and 12). Test RC-8 had a maximum end moment of  $M_o/M_p = 0.186$ , about 28% below "in-plane" ultimate moment and test RC-9 reached  $M_o/M_p = 0.542$ , within 4% of its "in-plane" value. Important to note is the relatively larger rotation capacity obtained for the A36 specimens despite the fact that the beam-columns had buckled, as compared with the sudden drop off which was observed for the A441 beam-column in test HT-40 (Figure 10).

Subassembly behavior was explained briefly in chapter 2 and a more comprehensive treatment is presented in Reference 7. Figure 13 presents the theoretical and experimental curves for test RC-10. The beam formed a plastic hinge and continued to rotate at a constant moment. The column buckled however and as a result, the structure supported an end moment of  $M_o/M_p = 0.774$ , 5% below the "in-plane" prediction of  $M_o/M_p = 0.814$ .

Two dial gages mounted on the testing machine and connected to the two flange tips by means of thin wire measured the lateral movement at mid-height of the column for the four unbraced beam-columns. The difference of the two dial gage readings gave the lateral movement of the compression flange tip with respect to the tension flange tip.

Assuming that no change in the shape of the cross section took place, the relative lateral movement was then divided by the depth of the section to obtain the twist. Figure 14 presents the moment-versus-twist curves for the four unbraced tests. The slopes of the moment-twist curves for the three unbraced A36 specimens were the same before each of the beam-columns in turn began to support a fairly constant centerline moment. The centerline moment is the sum of the applied moment and the axial load times the centerline deflection. The twists for the A36 specimens were much greater than that of the A441 specimen. At the end of the tests the A441 beam-column twisted about 0.046 radians and the three A36 beam-columns had each twisted more than 0.10 radians. The lateral deflection readings were not carried far enough to record the drop-off in load in any of the tests.

### 3.2 INFLUENCE OF THE AXIAL FORCE

Figure 15 presents a comparison of tests RC-8 and RC-9. The two beam-columns were identical. Both were 8WF31 beam-columns rolled from A36 steel and the nominal slenderness ratio in each case was 50. The variable parameter was the axial load ratio  $P/P_y$ . Test RC-8 had an actual  $P/P_y$  equal to 0.605 while test RC-9 supported a  $P/P_y$  equal to 0.312. The end moment which test RC-9 was able to support was 2.92 times that of test RC-8 while its axial load ratio was about half of that of RC-8. Due to the high axial load, yielding was observed in test RC-8 before the application of end moments and twisting was observed four increments later. In test RC-9, however, twisting was observed at the same moment application when first yield was observed.

### 3.3 INFLUENCE OF LATERAL-TORSIONAL BUCKLING

It was pointed out in Reference 6 that the effects of lateral-torsional buckling are most pronounced for a beam-column loaded with axial load and equal end moments causing single curvature deformation. In Figure 16 the moment-versus-rotation curves for two identical columns (HT-39 and HT-40) are shown. Both 8WF31 columns were rolled from A441 steel, both had a nominal slenderness ratio equal to 80, and the axial load ratio was approximately the same for each beam-column. Test HT-39 was provided with sufficient lateral bracing, whereas test HT-40 was not braced. It is seen from Figure 16 that the unbraced column was weaker despite the fact that it had a somewhat smaller axial force. It is interesting to note the sudden drop in load carrying capacity of test HT-40 as compared with that of tests RC-8 and RC-9 (Figure 15).

Tests RC-3 and RC-10 were also identical, with the variable parameter being the lateral bracing. They were each rolled from A36 steel, had approximately the same axial load ratio and the same slenderness ratio (Table 3). In each case joint restraint was provided by 8 ft. restraining beams. Test RC-3 was braced and test RC-10 was not. Figure 17 shows that in both tests the restraining beams (5WF18.5) carried approximately the same moment. The specimen in test RC-10 failed by lateral-torsional buckling therefore the beam-column was able to support less load than the beam-column in test RC-3. However, the difference in the behavior of the whole subassembly was not significant as is evident from Figure 17. The beam-columns buckled locally in the compression flange as the last increment of load was applied in both tests (Figure 17).



#### 4. COMPARISON OF THE TEST RESULTS WITH THEORY

In this chapter the test results will be compared with an inelastic lateral-torsional buckling theory<sup>(12)</sup> and with the inelastic column theory where failure is assumed by bending.<sup>(4)</sup>

##### 4.1 COMPARISON WITH INELASTIC LATERAL-TORSIONAL BUCKLING THEORY

The lateral-torsional buckling theory presented in Reference 12 includes the influence of cooling residual stresses. A typical symmetrical pattern of residual stress is assumed with maximum assumed compressive residual stress  $\sigma_{rc}$  equal to  $0.3\sigma_y$ .<sup>(13)</sup>

Coupled differential equations which involve lateral deflection and torsional deformation are presented in Reference 12. For the loading condition of axial load and equal end moments causing single curvature the eigenvalue solution of the coupled differential equations is:

$$\left[ P - \frac{\pi^2 B_y}{L^2} \right] \left[ P r_o^2 - C_T - \frac{\pi^2 C_w}{L^2} \right] - P^2 (e_y - y_o)^2 = 0 \quad (1)$$

After substitution of the expressions developed for the various coefficients<sup>(12)</sup> and after the performance of some algebraic manipulations and rearrangement, the following equation evolves

$$\begin{aligned} & \left\{ \left( \frac{P}{P_y} \right)^2 \left[ \left( \frac{r_o}{d} \right)^2 - \left( \frac{Z}{Ad} \frac{M_o}{M_p} + \Omega \right)^2 \right] - \frac{P}{P_y} \left( \frac{GK_T}{A\sigma_y d^2} \right) \right\} \left( \frac{L}{r_y} \right)^4 + \\ & + \frac{\pi^2 E}{\sigma_y} \left\{ \frac{GK_T B_1}{A\sigma_y d^2} - \frac{P}{P_y} \left[ \left( 1 - \frac{t}{d} \right)^2 B_2 + B_1 \left( \frac{r_o}{d} \right)^2 \right] \right\} \left( \frac{L}{r_y} \right)^2 + \\ & + \left( \frac{\pi^2 E}{\sigma_y} \right)^2 \left( 1 - \frac{t}{d} \right)^2 B_1 B_2 = 0 \quad (2) \end{aligned}$$

In this equation  $Z$ ,  $A$ ,  $d$ ,  $K_T$ ,  $r_y$  and  $t$  are properties of the cross section and  $E$ ,  $G$ , and  $\sigma_y$  are material properties.  $B_1$ ,  $B_2$ ,  $(r_o/d^2)$ , and  $\Omega$  are functions of the yielded cross section and are therefore functions of the applied axial load,  $P$  and the applied end moment,  $M_o$ .

In the development of Equation (2), it is assumed that lateral-torsional buckling occurs before the beam-column deforms very much. This assumption was necessary because in order to use Equation (1) the stiffnesses along the length of the beam-column were taken as uniform and equal to the stiffnesses which exist at the ends. In the case of a slender column loaded with a substantial axial force however, (e.g. test RC-8), large deformation and considerable yielding result at the mid-height of the beam-column. The result is a reduction in stiffness which is not accounted for by the stiffness coefficients,  $B_1$ ,  $B_2$ ,  $(r_o/d^2)$ , and  $\Omega$  in Equation (2). This reduction of stiffness is considerable and can not be neglected if a satisfactory solution is to be obtained.

If values of  $M_o/M_p$  are assumed and the various constants and coefficients evaluated, <sup>(12)</sup> Equation (2) can be solved for the corresponding values of  $L/r_y$ . The  $M_o/M_p$ -versus- $L/r_y$  curve can then be plotted. The end fixtures used for all tests in this series prevented rotation of the beam-column end about the weak axis. The effective length in the weak direction may therefore be taken as six tenths of the beam-column length ( $L_{eff.} = 0.6L$ ). <sup>(6)</sup> As a result, the corresponding

value of  $M_o/M_p$  may be found from the above drawn curve by using a slenderness ratio equal to six tenths of the weak axis slenderness ratio ( $L/r_{y \text{ eff.}} = 0.6 L/r_y$ ). This value of  $M_o/M_p$  can then be multiplied by the plastic moment,  $M_p$  and the value of  $M_o$  obtained is an upper bound solution since the variation of stiffness along the length of the beam-column was not considered and the mid-height stiffness was assumed to equal the end stiffness. A lower bound solution may now be obtained by using the appropriate column deflection curve<sup>(5)</sup> or nomograph<sup>(10)</sup> to find the corresponding end moment, if it is assumed that the end moment obtained from the upper bound solution is now the centerline moment. Figure 18 diagrammatically shows the significance of the upper and lower bound solution. A flow chart outlining the method for determining the two bounds is presented in Figure 19. Using lateral-torsional buckling theory<sup>(12)</sup> along with the column deflection curves<sup>(5)</sup> or nomographs<sup>(10)</sup> it is therefore possible to obtain upper and lower bounds.

In practical situations the case of the slender beam-column with high axial load is not too frequently encountered and for more efficient beam-columns, the lower bound solution tends to approach the upper bound solution. Care should be exercised always however because direct application of the methods discussed in Reference 12 do tend to yield unconservative results. The lower bound should always be checked.

Figures 20 through 23 present graphically the location of each test with respect to its inelastic lateral-torsional buckling upper bound, inelastic lateral-torsional buckling lower bound, elastic lateral-torsional buckling curve and the "in-plane" ultimate strength curve. It is important to note that in each case the "in-plane" ultimate strength curve crossed the inelastic lateral-torsional buckling upper bound thereby becoming the upper bound for the beam-column if its  $L/r_x$  was greater than that at the common point. This was the case for test HT-40 (Figure 20).

The elastic lateral-torsional buckling curve was computed from the following equation as found in Reference 14:

$$\frac{M_o}{M_p} = \sqrt{\frac{I_x + I_y}{Z} \left( \frac{P}{P_y} - \frac{P_y}{P_y} \right) \left( \frac{P}{P_y} - \frac{P_T}{P_y} \right)} \quad (3)$$

where

$$\frac{P_y}{P_y} = \frac{\pi^2 E}{\sigma_y} \cdot \frac{1}{\left(\frac{L}{r_y}\right)^2}$$

$$\frac{P_T}{P_y} = \left(\frac{E}{\sigma_y}\right) \left( \frac{I_w}{r_y^2 [I_x + I_y]} \right) \left[ \frac{\pi^2}{(L/r_y)^2} + \left(\frac{G}{E}\right) \left( \frac{K_T r_y^2}{I_w} \right) \right]$$

Table 5 presents a comparison of the experimental results with theory. The test moment is given and the upper bound and lower bound solutions for the particular  $L/r_x$  of the specimen are included. Test HT-39 failed by excessive bending so the lateral buckling theory does not apply. The maximum end moment obtained in test HT-40 was 337 kip in.

The upper bound solution yielded 518 kip in. and the lower bound was 240 kip in. As can be seen from the results the upper bound solution predicted 181 kip in. more than were actually obtained. This is 53.7% unconservative. Test RC-8 (a moderately slender column with a high axial load) failed at approximately the lower bound, 208 kip in., whereas test RC-9 (a moderately slender column with low axial load) failed at about its upper bound, 591 kip in. The upper bound in test RC-10 proved to be 13.5% unconservative.

#### 4.2 COMPARISON WITH BENDING THEORY

Figures 20 through 23 show that when the slenderness ratio  $L/r_x$  gets large enough the "in-plane" ultimate strength curve becomes an upper bound. This curve is computed by using the bending theory<sup>(4)</sup> which assumes that failure is due to excessive bending in the applied moments. Since bending was about the strong axis this would be in the plane of the web in this case. The influence of cooling residual stresses is included in the theory as it was in the lateral-torsional buckling theory (that is, a symmetrical pattern is assumed with  $\sigma_{rc}$  equal to  $0.3\sigma_y$ ). Interaction curves which relate axial load, end bending moments, and slenderness ratio have been developed. These curves apply specifically to 8WF31 beam-columns rolled from ASTM-A7 steel with  $E = 30,000$  ksi and  $\sigma_y = 33$  ksi. If the material from which the beam-column is fabricated has a yield point other than 33 ksi, the slenderness ratio is modified. The adjustment is made using the following equation

$$\left(\frac{L}{r}\right)_{33} = \left(\frac{L}{r}\right)_y * \sqrt{\frac{\sigma_y^*}{33}} \quad (4)$$

In this equation  $\sigma_y^*$  is the yield point stress in kips per square inch of the test beam-column material.

In the AISC Specification<sup>(15)</sup>, formulas which are mathematical approximations to the interaction curves described above are given. They are applicable to A7 and A36 rolled WF members but here again modification may be made for higher strength steels by using Equation (4).

The formula for this case of loading is:

$$M_o = M_p \left[ 1.0 - K \left( \frac{P}{P_y} \right) - J \left( \frac{P}{P_y} \right)^2 \right] \quad (5)$$

where K and J are functions of the slenderness ratio and are given in tabularized form in the specifications.<sup>(15)</sup> The results are given in Table 5. For the braced column in test HT-39, Equation (5) proved to be 7.1% unconservative. For the other four tests the theory does not apply, as is seen by the unconservative comparison between test and theory.

5. COMPARISON OF THE TEST RESULTS  
WITH THE CRC INTERACTION EQUATION

The CRC Interaction equation is one that has been recommended for use and a comparison of this equation with the test results of the unbraced columns is worthwhile.

The basic equation in terms of ultimate strength as given by the CRC<sup>(16)</sup> is:

$$\frac{P}{P_u} + \frac{M}{M_{ul} \left(1 - \frac{P}{P_{el}}\right)} = 1 \quad (6)$$

where  $P_u$  is the collapse load for the column centrally loaded for buckling in the unconstrained plane and was determined from the smaller of the following two equations

$$\frac{P_u}{P_y} = 1 - \frac{\sqrt{y}}{4\pi^2 E} \left(\frac{L}{r_x}\right)^2 \quad (7a)$$

or

$$\frac{P_u}{P_y} = 1 - \frac{\sqrt{y}}{4\pi^2 E} \left(\frac{0.6L}{r_y}\right)^2 \quad (7b)$$

Equation (7a) reflects the possibility of strong axis buckling and (7b) reflects the possibility of weak axis buckling.  $P_{el}$  is the strong axis Euler load and  $M_{ul}$  is a reduced inelastic moment which is determined by using the moment reduction curve in Reference 17. The moment to be reduced is determined by the following equation:

$$M_u = \frac{\pi}{L} \sqrt{EI_y GK_T} \sqrt{1 + \frac{\pi^2 EI_w}{(0.6L)^2 GK_T}} \quad (8)$$

Table 5 presents the results of the CRC equation compared with the experimental values for each of the unbraced tests. In tests RC-9 and RC-10, the agreement was very good. In test HT-40 the equation proved to be 22.3% conservative, but in test RC-8 it resulted in a 32% difference on the unconservative side. When the results are viewed in the light of Figure 24 which presents the results graphically, the differences between the experimental results and the CRC values are not too bad.

For test HT-39 the reduced inelastic moment,  $M_{ul}$  in Equation (6) is replaced by the plastic moment  $M_p$ , because the lateral bracing prevented lateral torsional buckling. The result for this test is also given in Table 5 and Figure 24.



## 6. SUMMARY AND CONCLUSIONS

The experiments discussed in this thesis were performed to study the strength and deformation behavior of unbraced wide-flange beam-columns rolled from ASTM A36 and A441 steels. The conclusions reached are as follows:

- (1) Unbraced beam-columns loaded with an axial load and equal end moments causing single curvature deflection fail by lateral-torsional buckling.
- (2) The reduction in rotation capacity because of lateral-torsional buckling appears to be greater for A441 beam-columns than for A36 beam-columns (Figures 10 and 12).
- (3) It was shown that strength and rotation capacity of unbraced columns increases as axial force decreases (Figure 15).
- (4) The unloading of an unbraced subassembly (consisting of a column with restraining beams) that is proportioned so that a plastic hinge forms in the beam before failure of the column will finally result from lateral-torsional buckling of the column.
- (5) A comparison with the "exact" lateral-torsional buckling theory (Reference 12) shows that direct application provides an upper bound and that for a relatively slender column with high axial load the result obtained may be unconservative (Table 5).
- (6) The "in-plane" ultimate strength curve<sup>(4) (11) (15)</sup> crosses the lateral-torsional buckling upper bound<sup>(12)</sup> and becomes an upper bound at slenderness ratios that are in the practical range.

(7) A comparison with the Column Research Council interaction equation (Equation 6) has shown that in all cases except the case of a relatively slender column with high axial load, (RC-8), the results obtained are adequate for design purposes.

7. N O M E N C L A T U R E

$A$	=	Cross sectional area
$B_1$	=	A bending stiffness coefficient
$B_2$	=	A warping stiffness coefficient
$B_y$	=	Bending stiffness about x-axis (weak axis stiffness)
$C_T$	=	St. Venant's torsional stiffness
$C_w$	=	Warping stiffness
$E$	=	Young's modulus of elasticity
$G$	=	Shear modulus
$I_x$	=	Moment of inertia about the x axis
$I_y$	=	Moment of inertia about the y axis
$I_w$	=	Warping moment of inertia
$K_T$	=	St. Venant's torsion constant
$L/r$	=	Slenderness ratio
$L/r_x$	=	Strong axis slenderness ratio
$L/r_y$	=	Weak axis slenderness ratio
$M$	=	Moment
$M_o$	=	Applied end bending moment
$M_p$	=	Full plastic moment of a cross section
$M_{ul}$	=	Reduced inelastic moment which can be carried in the absence of axial force
$M_y$	=	Moment at yield stress
$P$	=	Axial force applied to the column
$P_{el}$	=	Euler load in the plane of bending
$P_u$	=	Collapse load for the column centrally loaded for buckling in the unrestrained plane

- $P_y$  = Axial force causing uniform yielding of the cross section
- $S$  = Section modulus
- $Z$  = Plastic modulus
- $d$  = Depth of section
- $e_y$  = Moment lever arm
- $r_x$  = Radius of gyration about the x axis
- $r_y$  = Radius of gyration about the y axis
- $r_o/d$  = A coefficient appearing in the lateral-torsional buckling equation
- $t$  = Thickness of flange
- $y_o$  = Distance between centroid and shear center
- $\sigma_y$  = Yield stress
- $\Omega$  = An eccentricity coefficient
- $\theta$  = End rotation

8. TABLES AND FIGURES

TABLE 1 TESTING PROGRAM

TEST NO.	$P/P_y$	$L/r_x$	MATERIAL	REMARKS
HT-39	0.4	80	A441	BRACED BEAM-COLUMN
HT-40	0.4	80	A441	UNBRACED BEAM-COLUMN
RC-8	0.6	50	A36	UNBRACED BEAM-COLUMN
RC-9	0.3	50	A36	UNBRACED BEAM-COLUMN
RC-10	0.4	60	A36	UNBRACED RESTRAINED COLUMN
RC-3	0.4	60	A36	BRACED RESTRAINED COLUMN

TABLE 2 MEASURED CROSS SECTION PROPERTIES

TEST NO.	SECTION	A sq. in.	$S_x$ cu. in.	$Z_x$ cu. in.	$r_x$ inch	$r_y$ inch
HT-39	8WF31	9.43	27.3	30.9	3.43	1.95
HT-40	8WF31	9.58	28.0	31.2	3.45	1.96
RC-8	8WF31	9.93	28.7	32.0	3.44	1.94
RC-9	8WF31	9.93	28.7	32.0	3.44	1.94
RC-10	8WF31	9.90	28.8	32.5	3.45	2.00
RC-3	8WF31	9.78	29.2	32.8	3.50	2.00

TABLE 3 MATERIAL AND LENGTH PROPERTIES

TEST NO.	$y$ ksi	$P_y$ kips	$M_y$ in-kip	$M_P$ in-kip	L inch	$L/r_x$
HT-39	50.0	471	1365	1545	277.6	81.1
HT-40	52.3	501	1460	1626	277.6	80.5
RC-8	33.6	334	964	1075	173.5	50.5
RC-9	33.6	334	964	1075	173.5	50.5
RC-10	34.1	337	980	1108	208.1	60.5
RC-3	35.3	340	1030	1160	208.1	59.5



TABLE 4 EXPERIMENTAL RESULTS.

TEST NO.	$L/r_x$	P kips	$P/P_y$	$M_o$ max. in-kip	$\frac{M_o}{M_p}$ max.
HT-39	81.1	200	0.425	353	0.228
HT-40	80.5	200	0.400	337	0.208
RC-8	50.5	202	0.605	200	0.186
RC-9	50.5	104	0.312	583	0.542
RC-10	51.5	143.5	0.425	414	0.374
RC-3	50.8	141	0.416	489	0.421

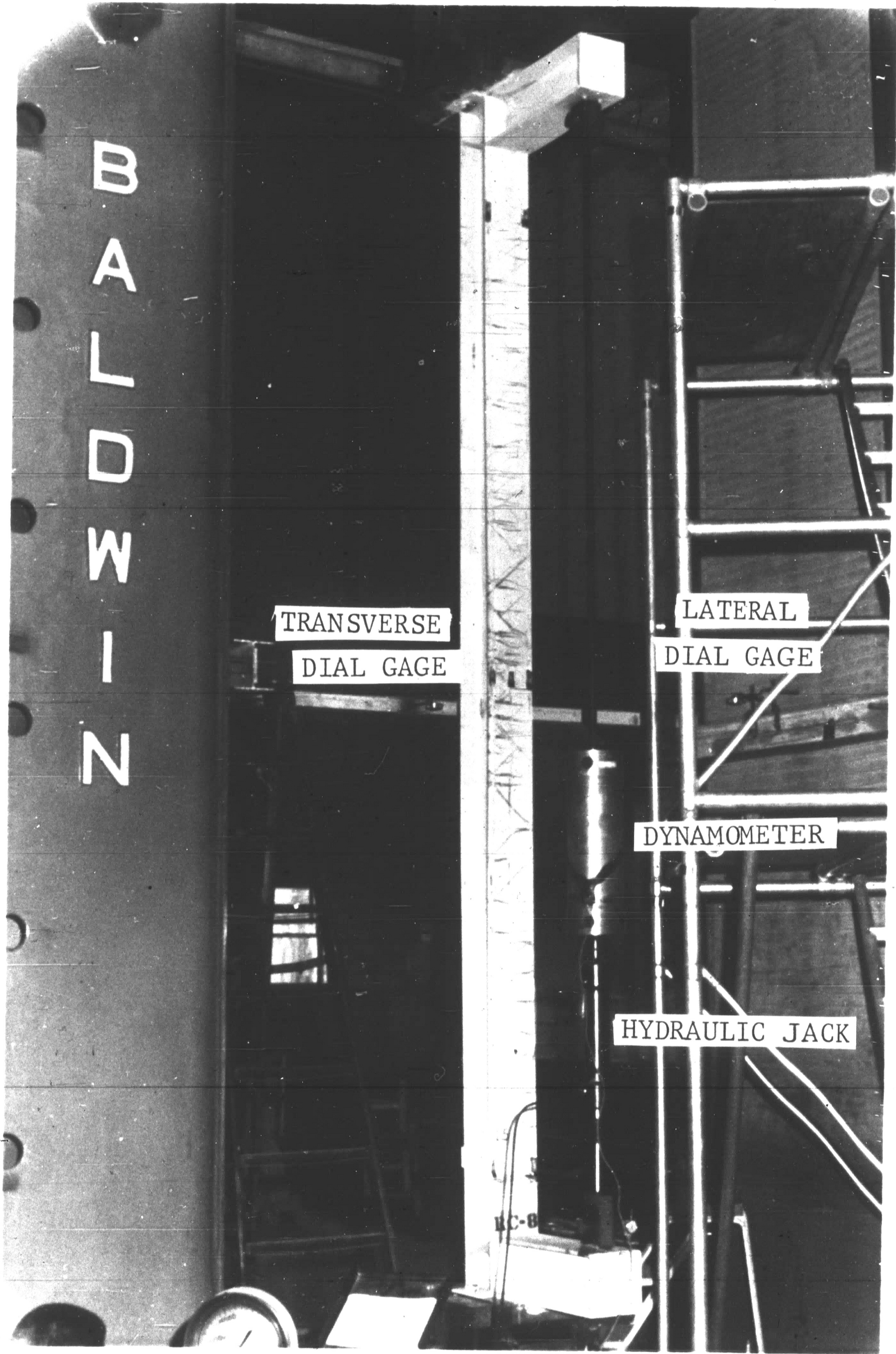
TABLE 5 COMPARISON OF EXPERIMENTS WITH THEORY

TEST NO.	HT-39	HT-40	RC-8	RC-9	RC-10
TEST MOMENT	353	337	200	583	414
LATERAL-TORSIONAL BUCKLING THEORY, UPPER BOUND		518	299	591	470
LATERAL-TORSIONAL BUCKLING THEORY, LOWER BOUND		240	208	528	387
CRC METHOD	329	262	264	571	411
INTERACTION (BRACED IN-PLANE BEHAVIOR)	378	437	314	681	548

All numbers are beam-column end moments with the units of kip-in.



FRONT VIEW OF A TYPICAL TEST SET-UP



REAR VIEW OF A TYPICAL TEST SET-UP

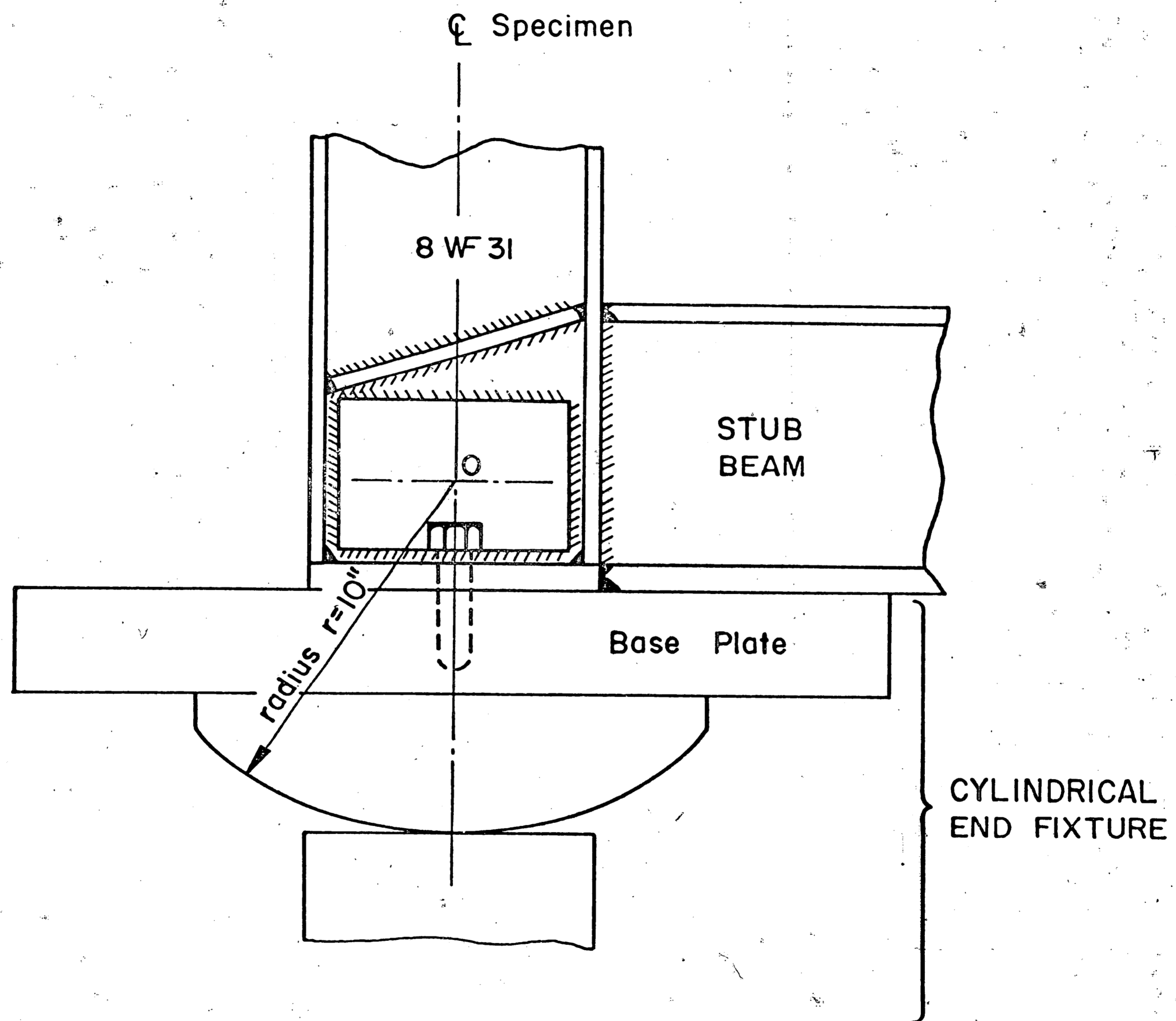


FIG. 3 CONNECTION AND END FIXTURE

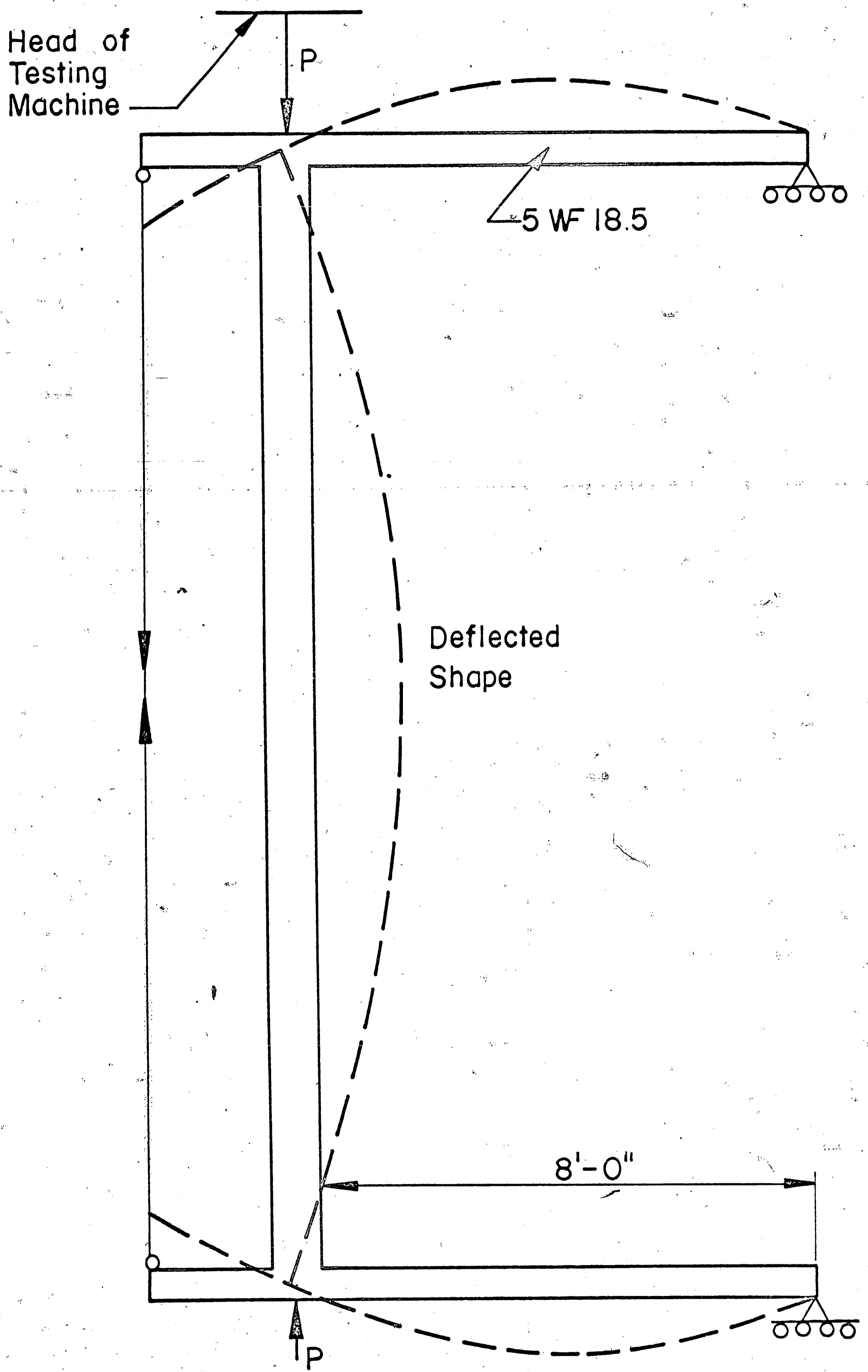


FIG. 4 TEST SUBASSEMBLAGE (RC-3 and RC-10)



RESTRAINED COLUMN END DETAIL

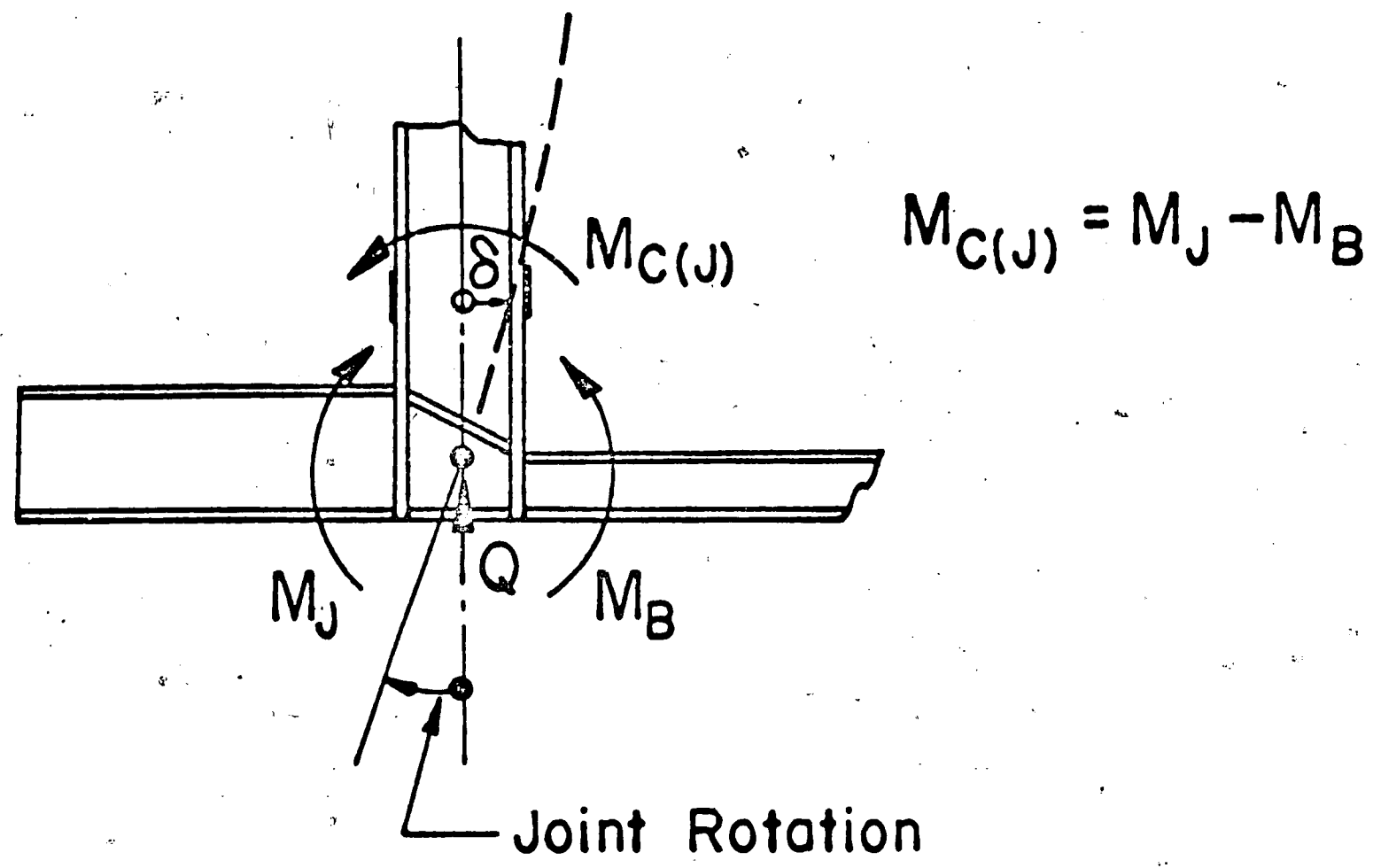


FIG. 6 JOINT MOMENTS

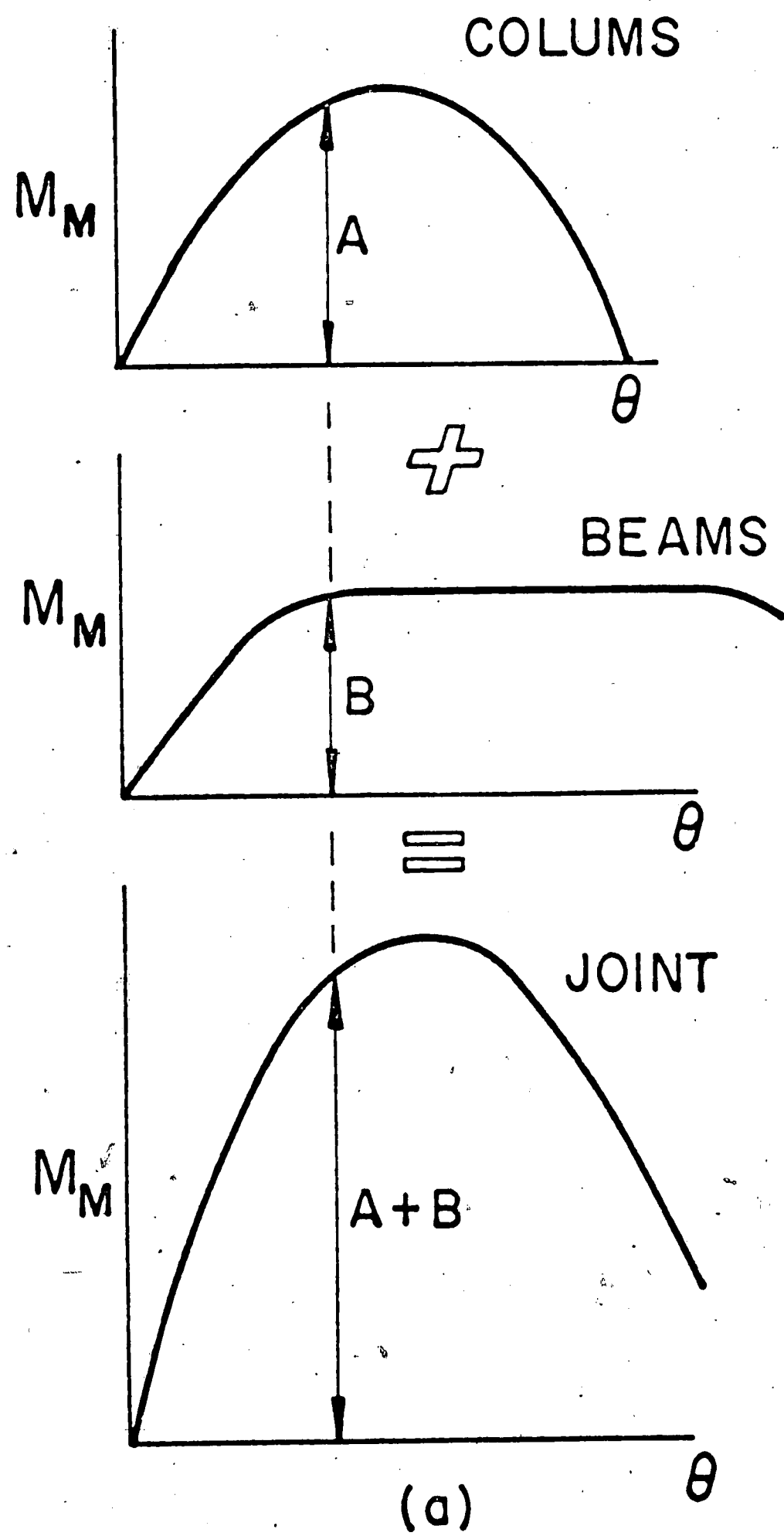


FIG. 7 BRACED JOINT



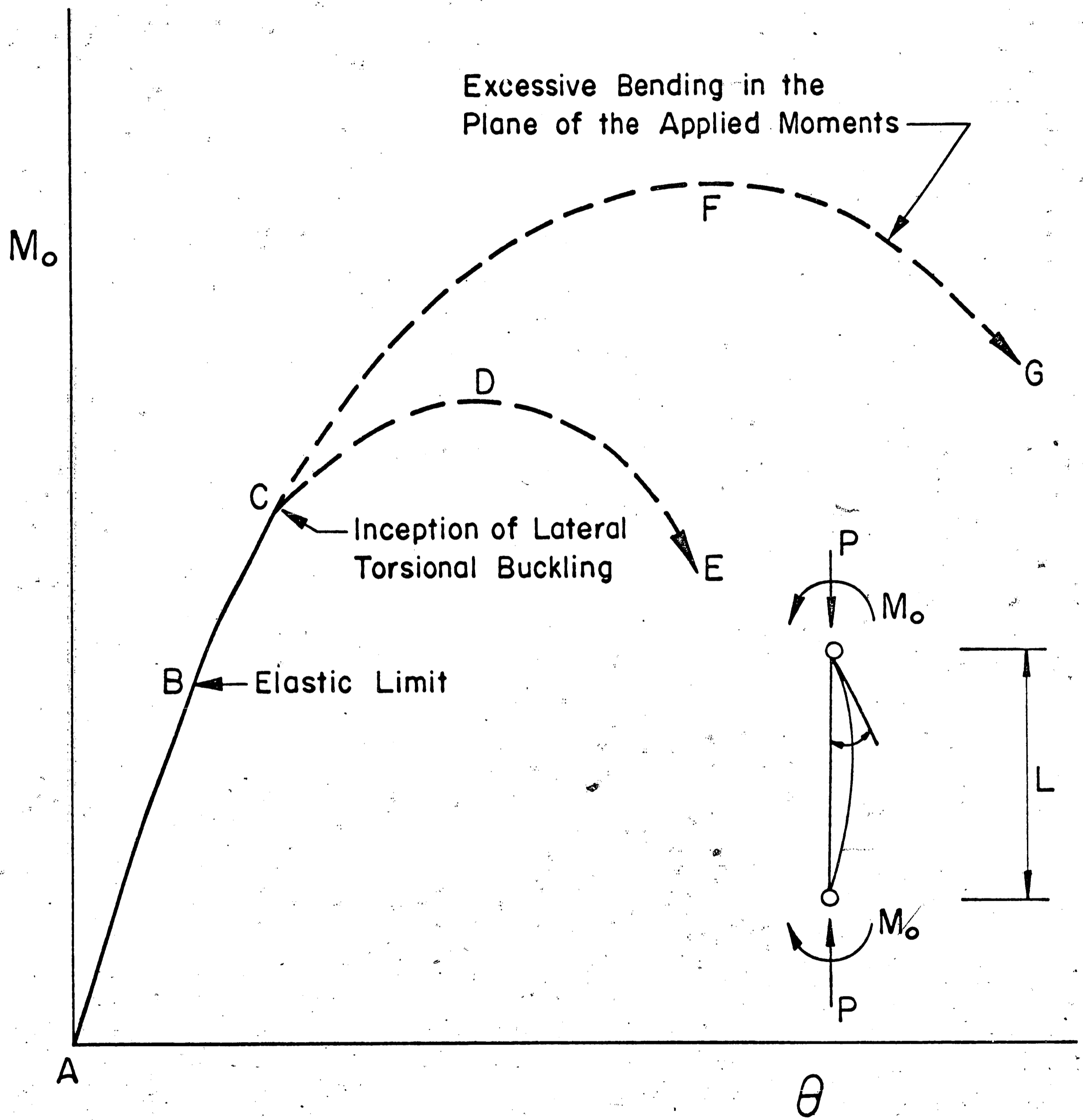


FIG. 8 EXCESSIVE BENDING AND LATERAL-TORSIONAL BUCKLING BEHAVIOR

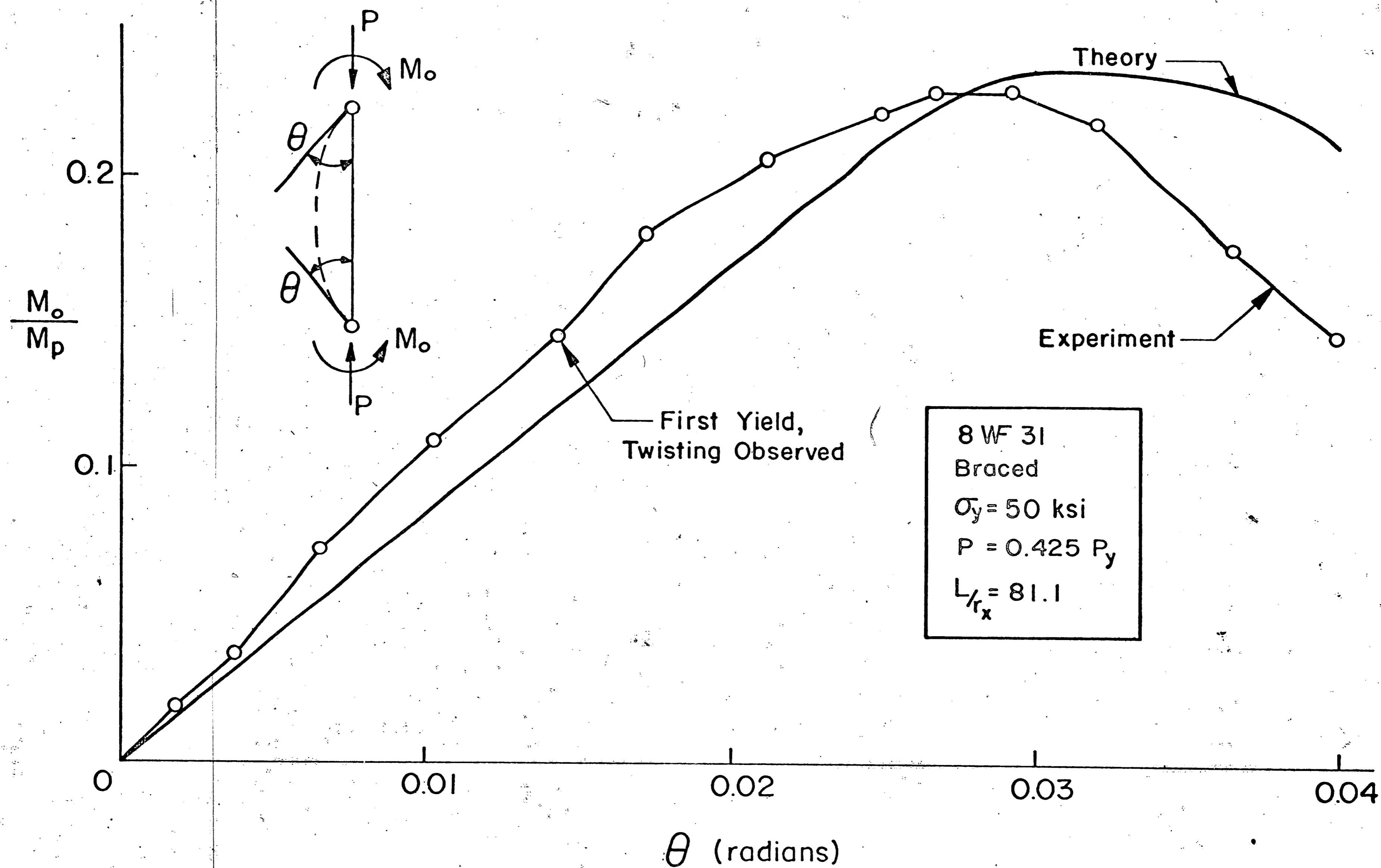


FIG. 9 TEST HT-39 EXPERIMENTAL RESULTS

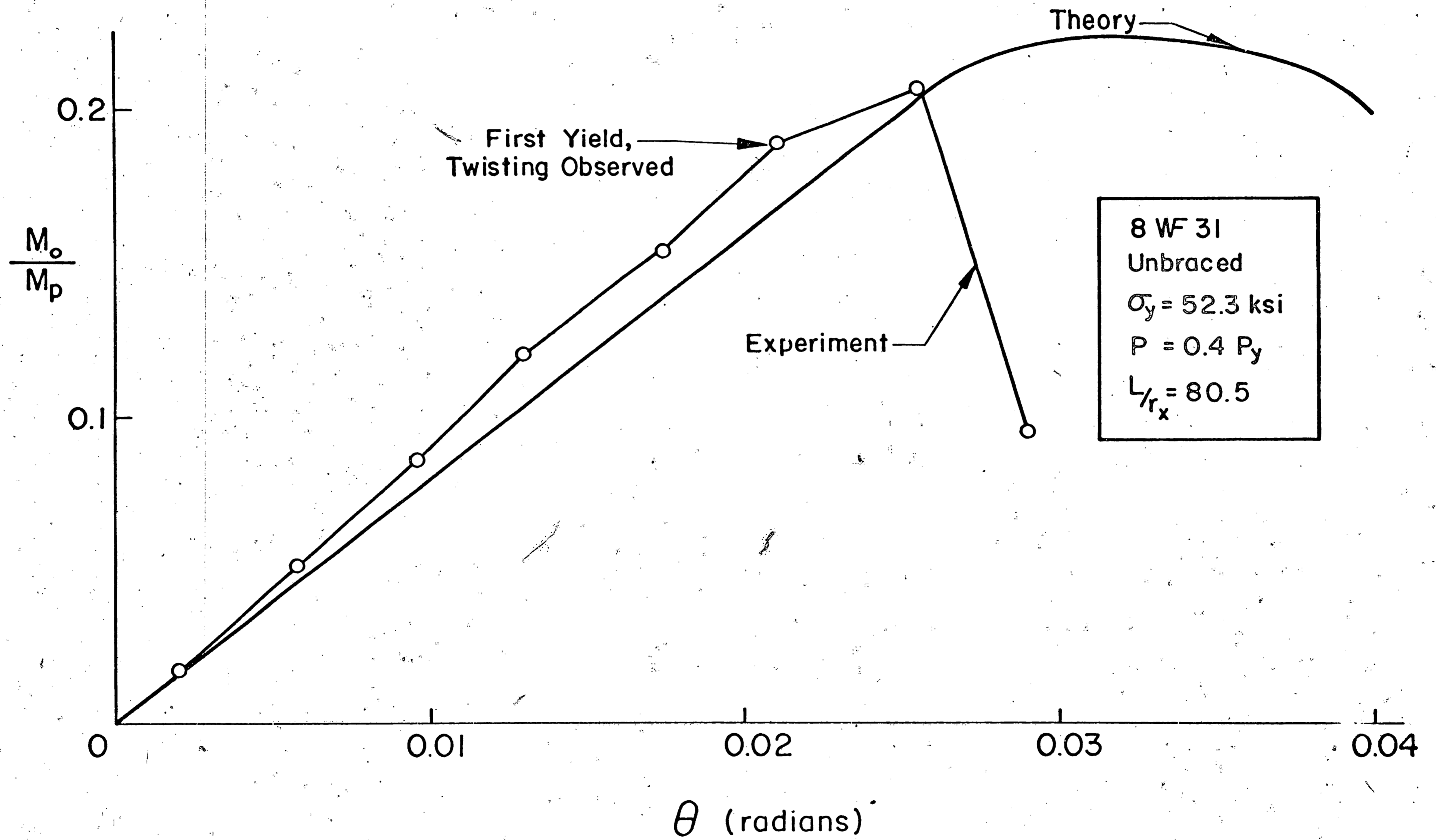


FIG. 10 TEST HT-40 EXPERIMENTAL RESULTS

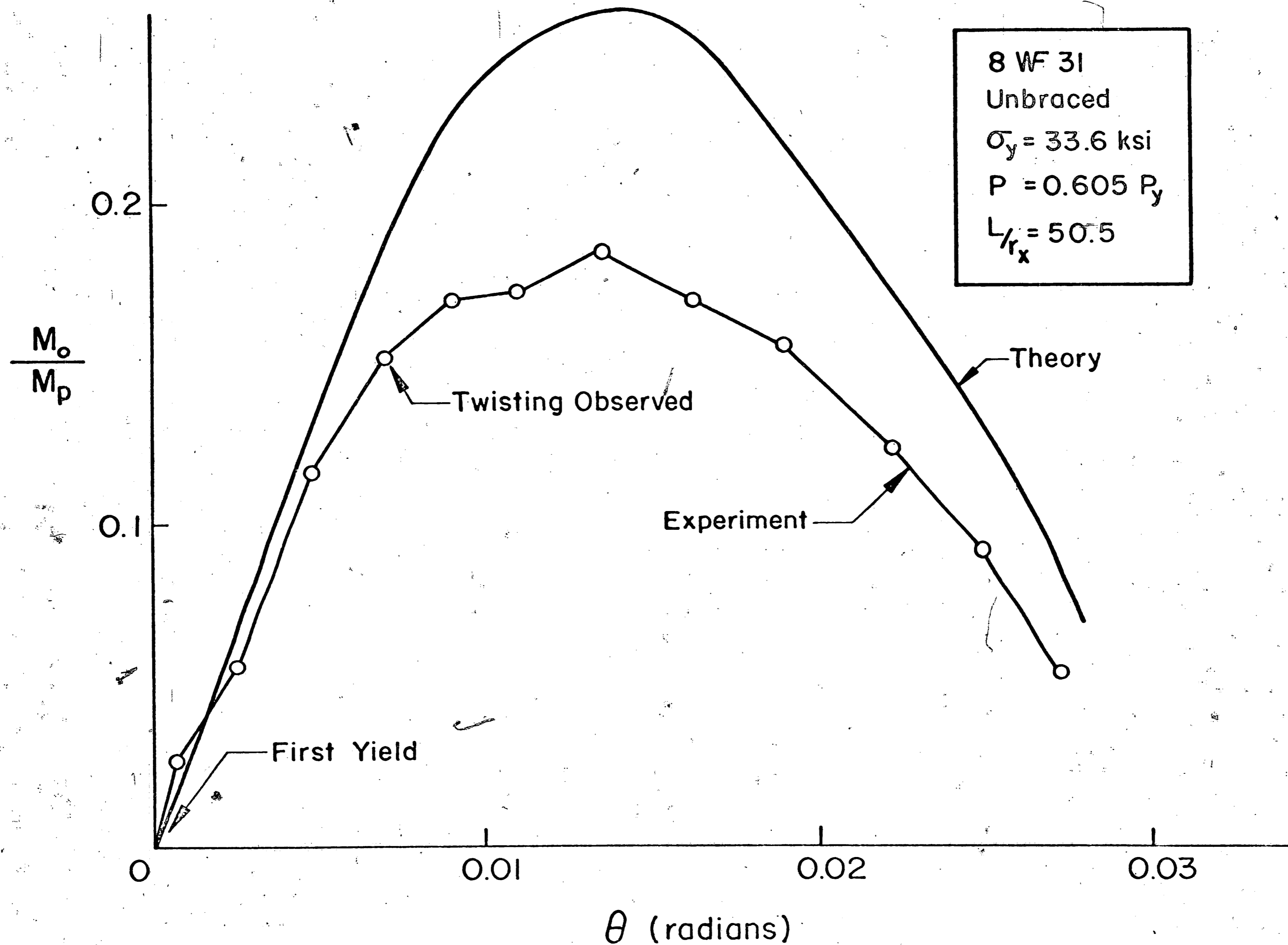


FIG. 11 TEST RC-8 EXPERIMENTAL RESULTS

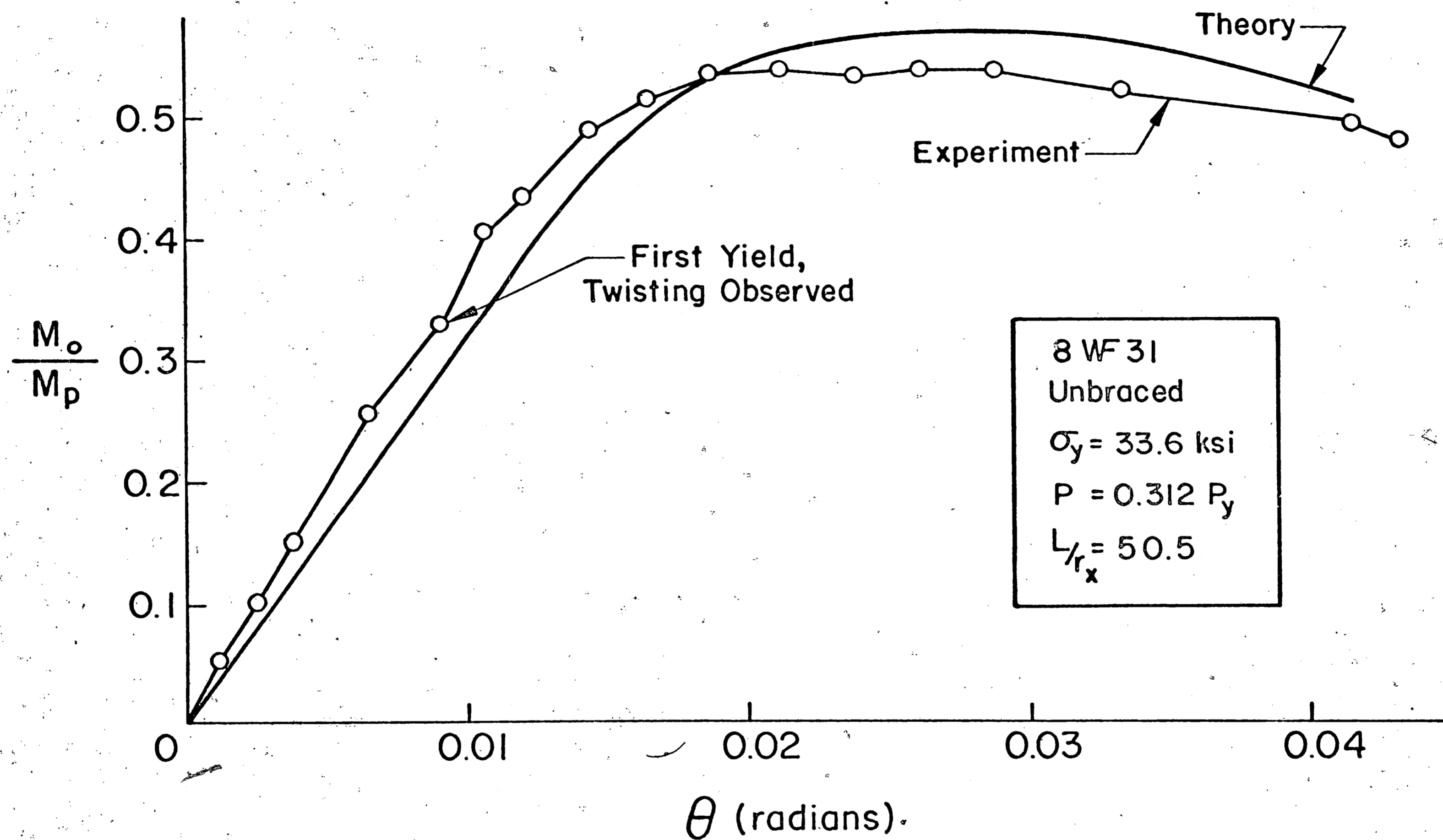


FIG. 12 TEST RC-9 EXPERIMENTAL RESULTS

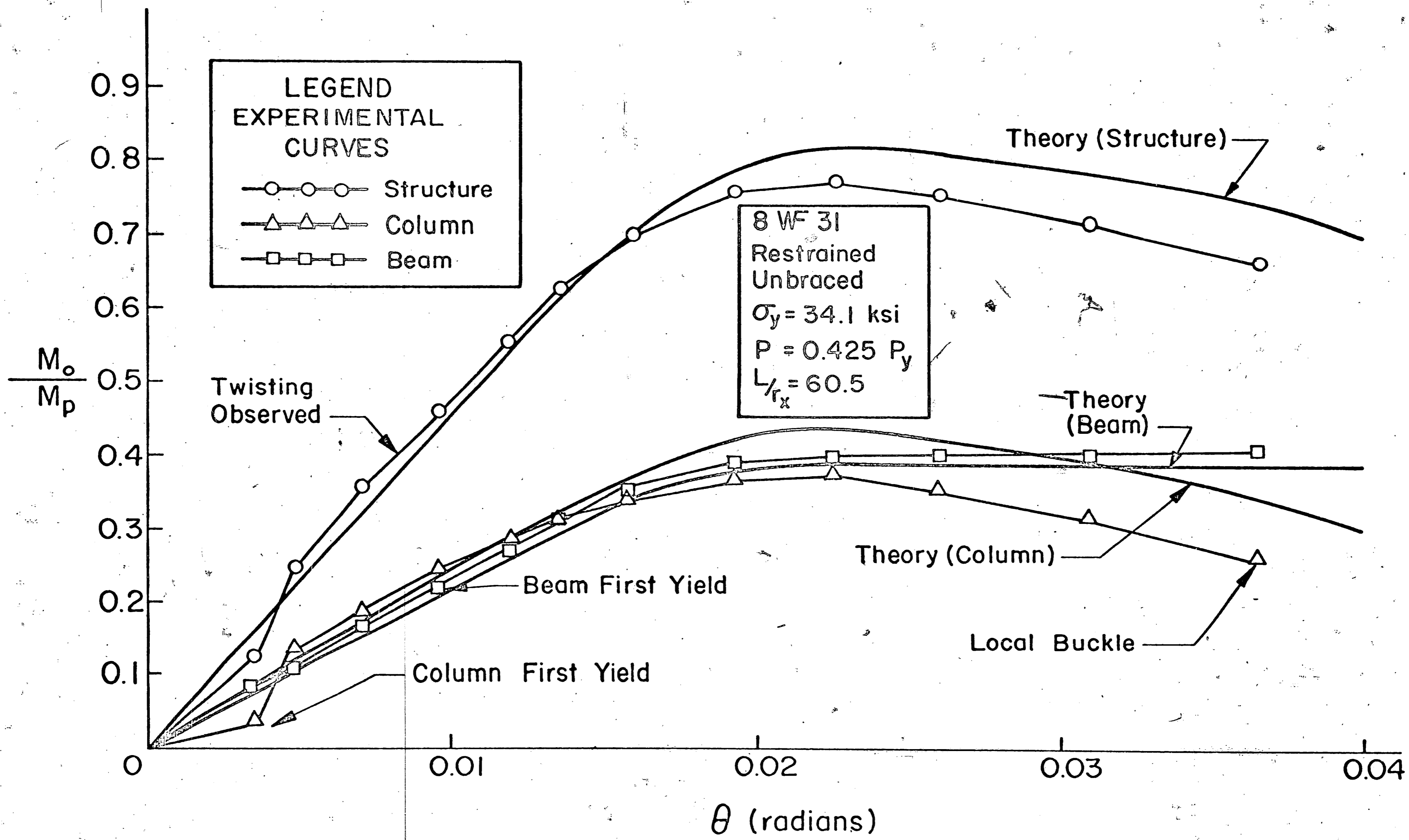


FIG. 13 TEST RC-10 EXPERIMENTAL RESULTS

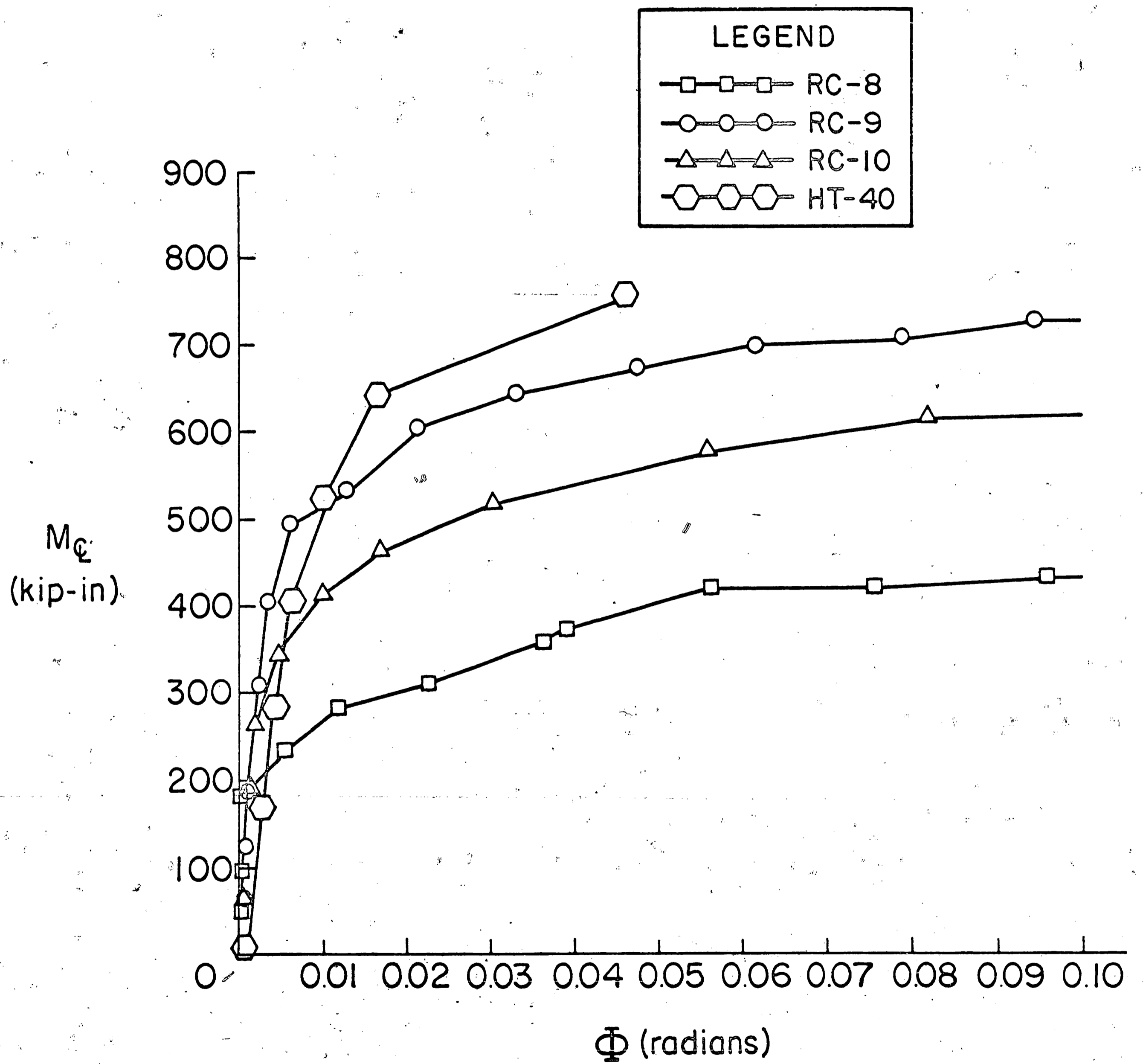


FIG. 14 MOMENT TWIST-CURVES

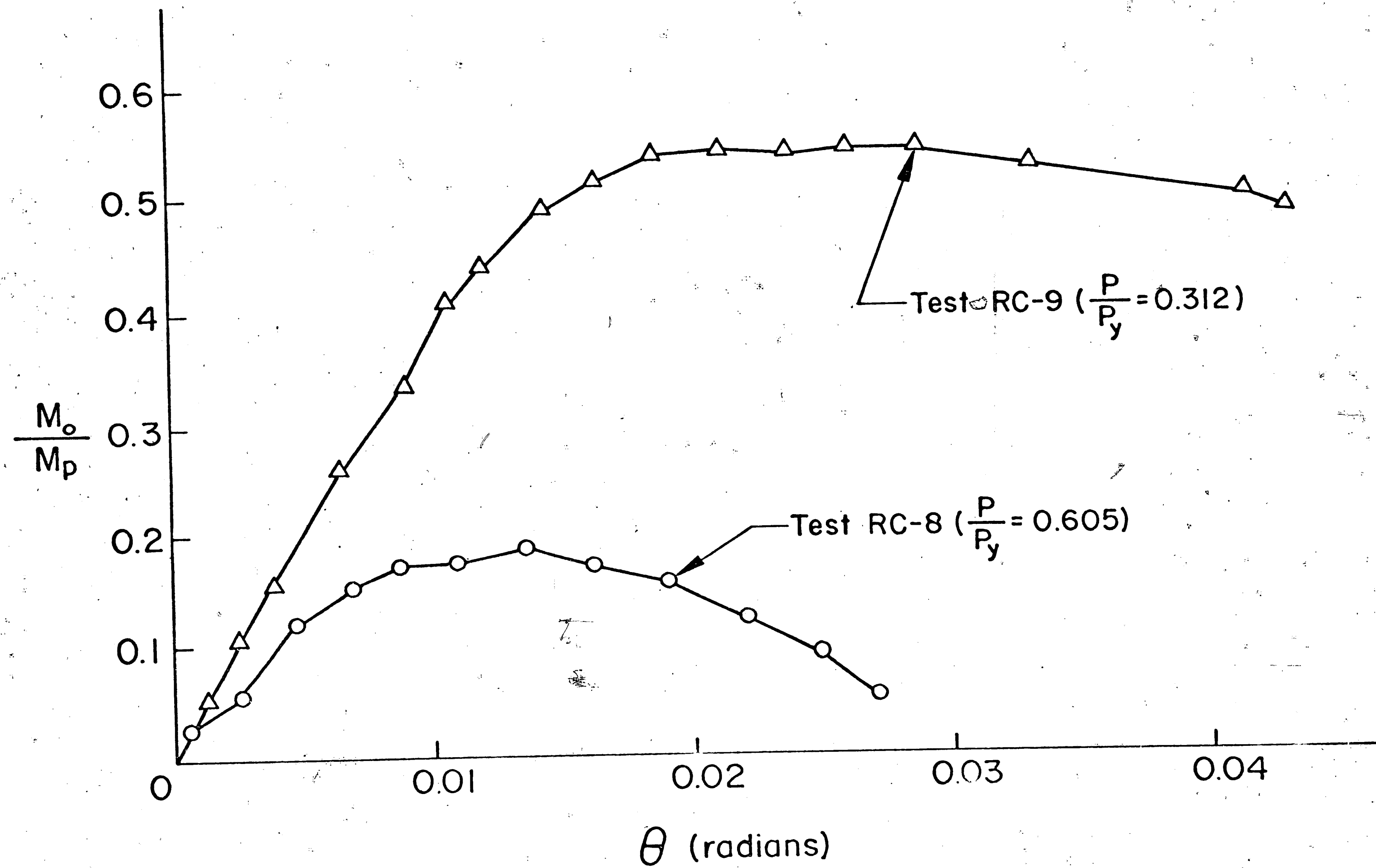


FIG. 15 RC-8 AND RC-9 COMPARISON CURVES



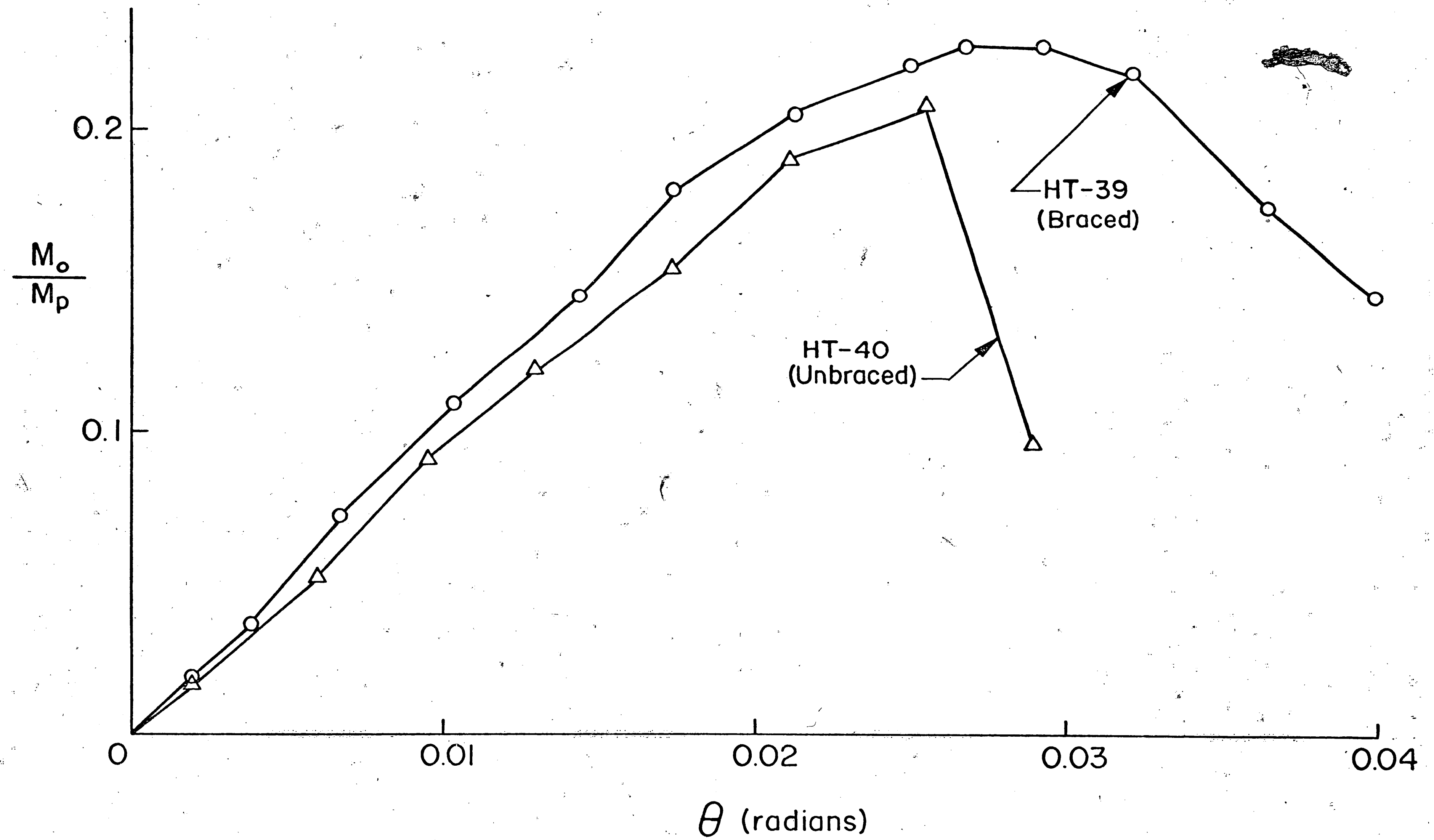


FIG. 16 HT-39 AND HT-40 COMPARISON CURVES

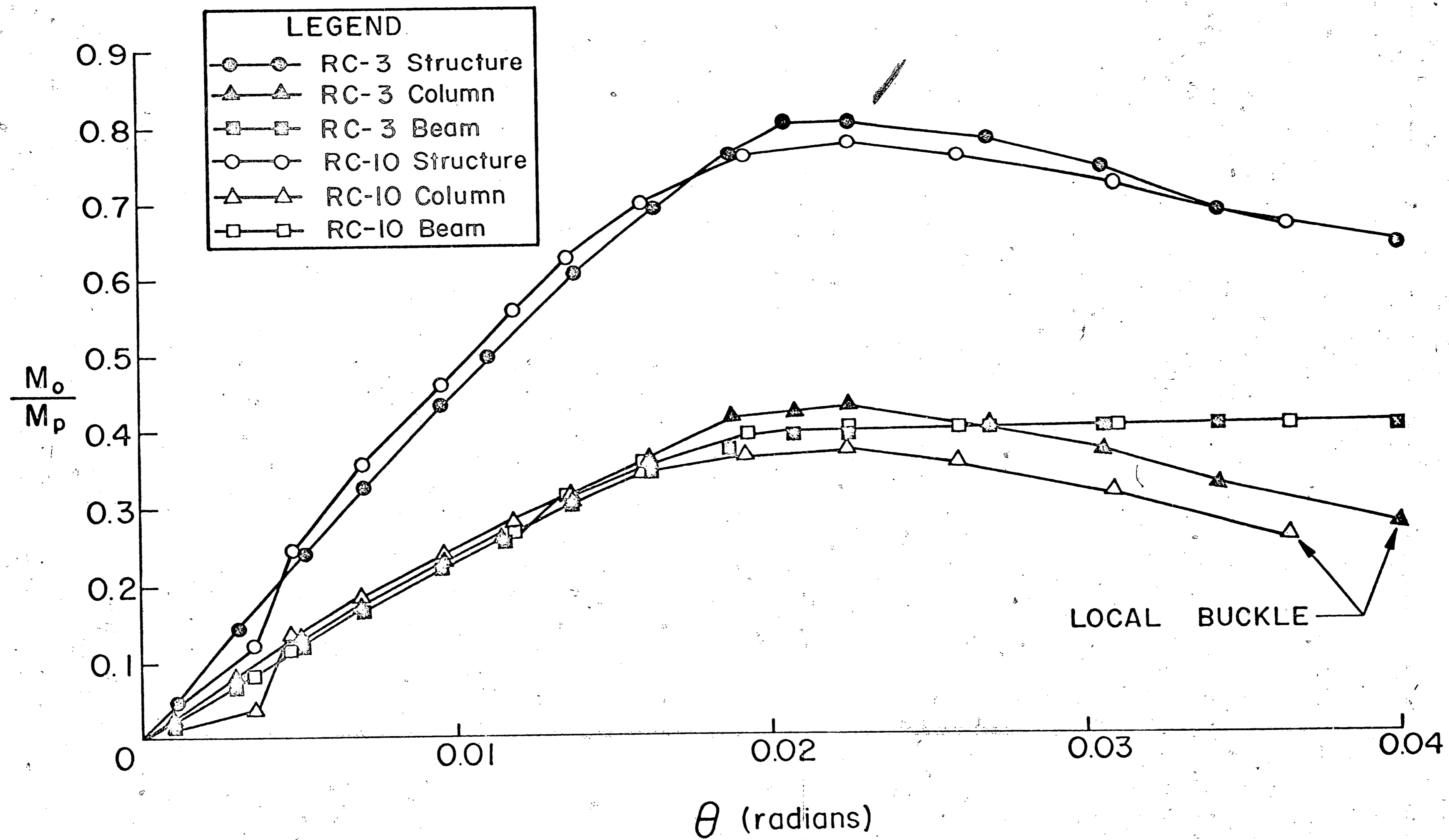


FIG. 17 RC-3 AND RC-10 COMPARISON CURVES

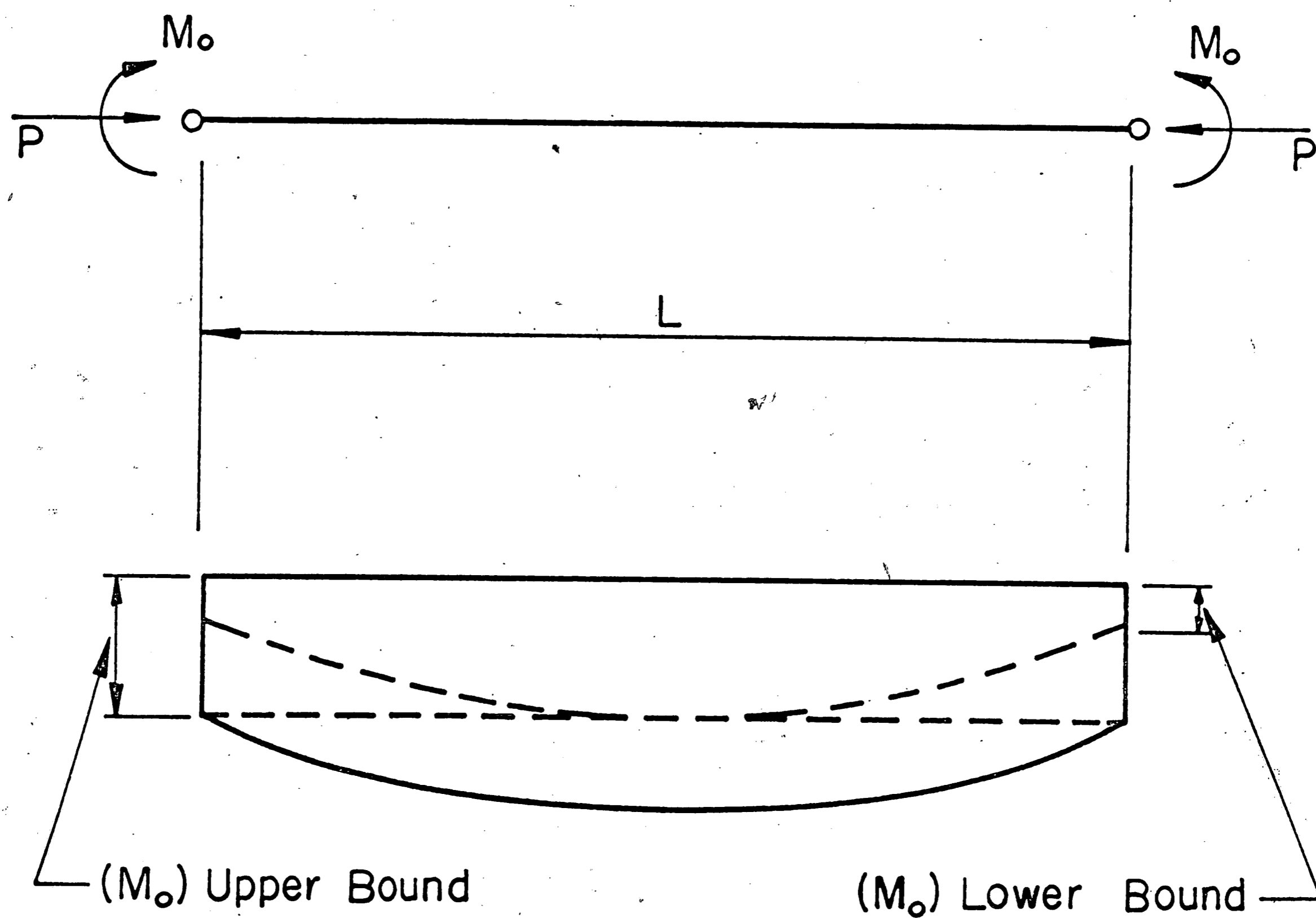


FIG. 18 UPPER BOUND AND LOWER BOUND MOMENT DIAGRAMS

Find  $(M_o)_{cr}$  for given  $L, P$ , material  
and cross section

- 1) Assume  $M_o$ , determine  $B_1, B_2, (\frac{r_o}{d})^2, \Omega$ , and solve for  $L$  from Eq. 2
- 2) Assume new values of  $M_o$ , until a  $M$  versus  $L$  curve can be constructed
- 3) For the given  $L$ , obtain  $(M_o)_{cr}$  from this curve  
 $(M_o)_{cr} \equiv$  Upper Bound

- 1) Set  $(M_o)_{cr}/U.B. = M$  at center of member
- 2) From CDC find  $M_o$  corresponding to this moment

$M_o \equiv$  Lower Bound

FIG. 19 UPPER AND LOWER BOUND FLOW SHEET

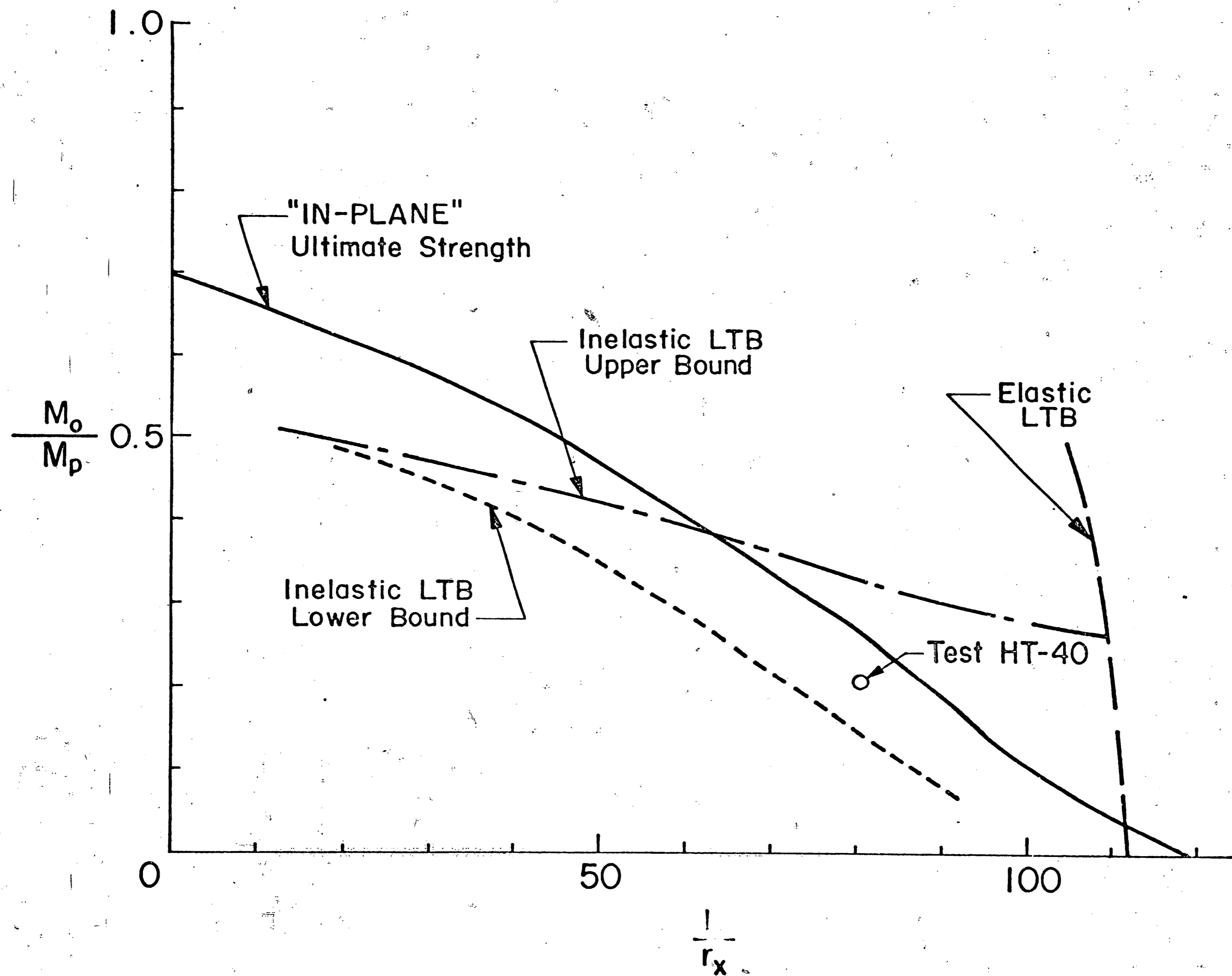


FIG. 20 COMPARISON OF HT-40 WITH THEORY

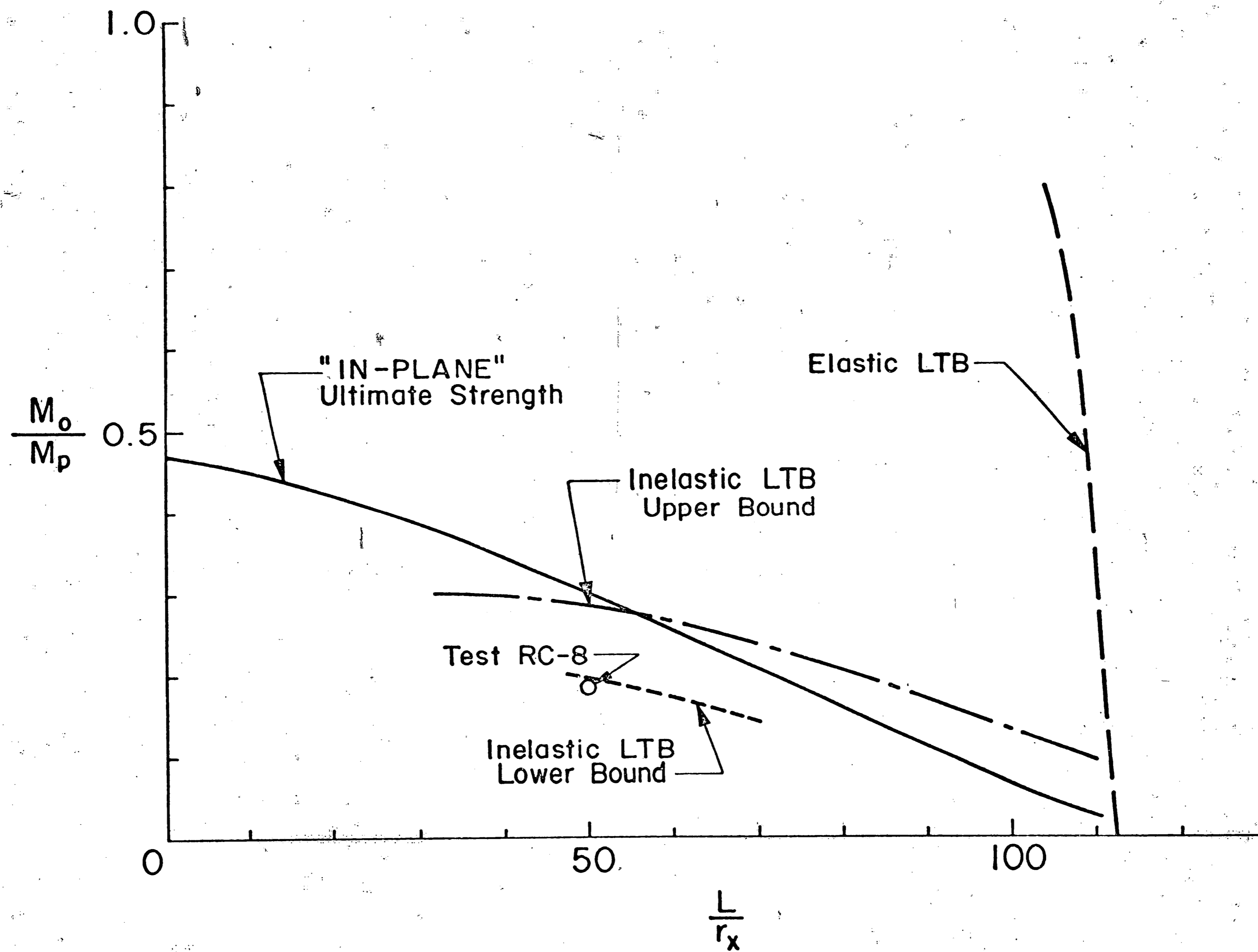


FIG. 21 COMPARISON OF RC-8 WITH THEORY

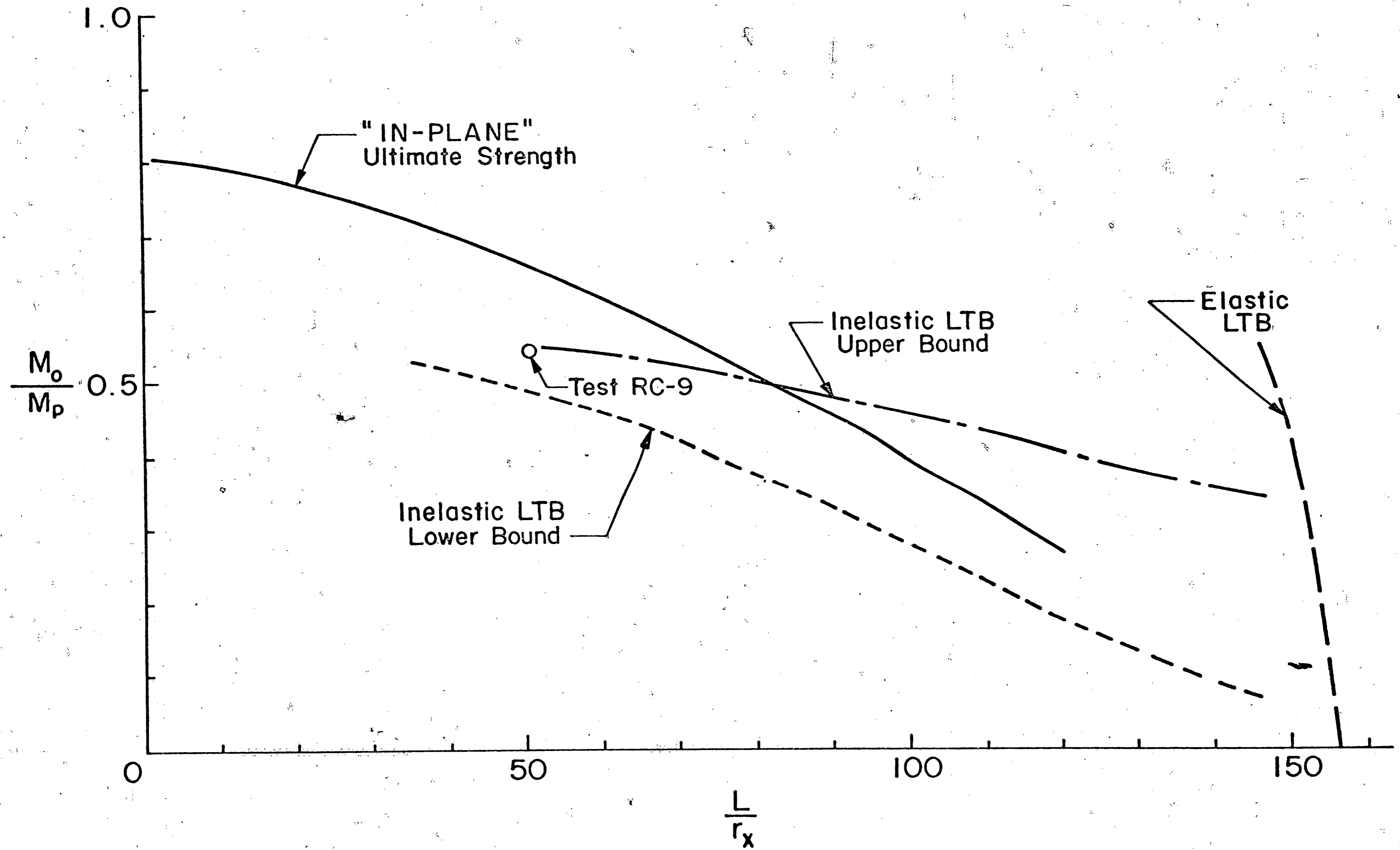


FIG. 22 COMPARISON OF RC-9 WITH THEORY

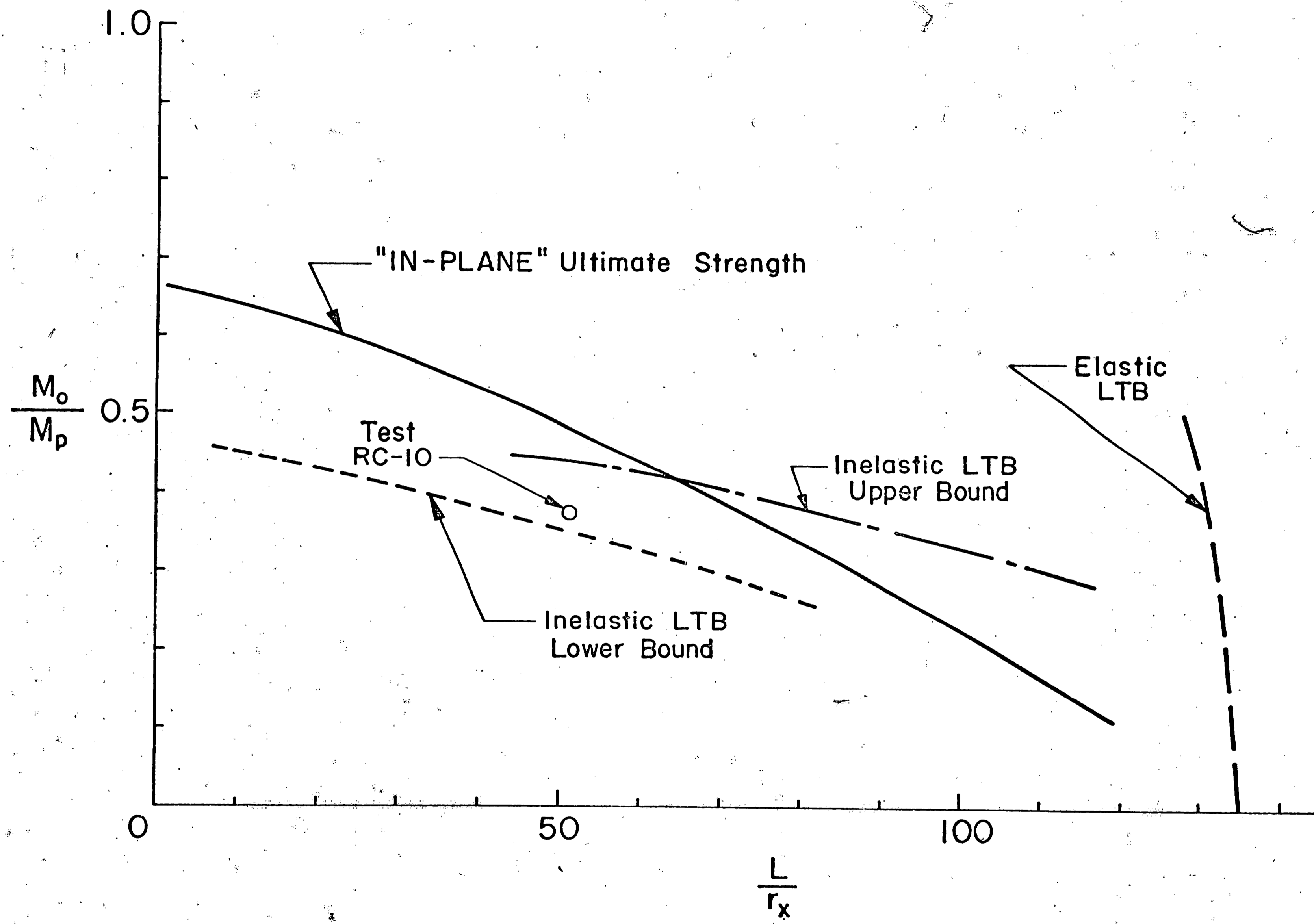


FIG. 23. COMPARISON OF RC-10 WITH THEORY



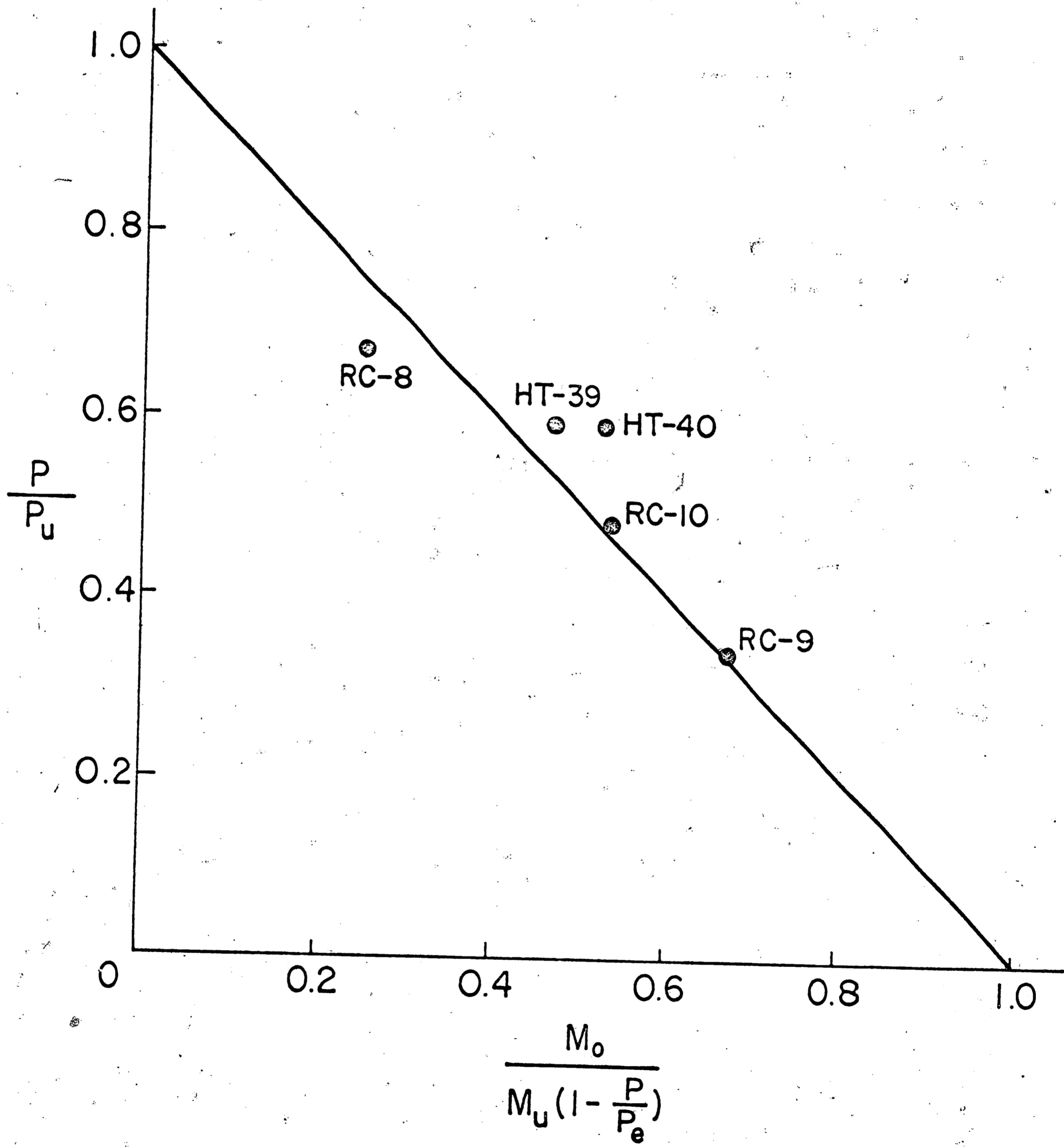


FIG. 24 COMPARISON OF TESTS WITH THE CRC INTERACTION EQUATION

## 9. REFERENCES

1. Ojalvo, M. and Lu, L. W.  
ANALYSIS OF FRAMES LOADED INTO THE PLASTIC RANGE  
Proc. ASCE, Vol. 87, EM4, August 1961
2. Ojalvo, M. and Levi, V.  
COLUMN DESIGN IN PLANAR CONTINUOUS STRUCTURES  
Proc. ASCE, Vol. 89, ST1, February 1963
3. Levi, V.  
PLASTIC DESIGN OF MULTI-STORY BRACED FRAMES  
Ph.D. Dissertation, Lehigh University, 1962  
(University Microfilms, Ann Arbor, Michigan)
4. Galambos, T. V. and Ketter, R. L.  
COLUMNS UNDER COMBINED BENDING AND THRUST  
Trans. ASCE, Vol. 126 (I), p. 1, 1961
5. Ojalvo, M.  
RESTRAINED COLUMNS  
Proc. ASCE, Vol. 86, EM5, October 1960
6. Van Kuren, R. C. and Galambos, T. V.  
BEAM-COLUMN EXPERIMENTS  
Proc. ASCE, Vol. 90, ST2, April 1964
7. Lay, M. G.; Aglietti, R. A. and Galambos, T. V.  
TESTING TECHNIQUES FOR RESTRAINED BEAM-COLUMNS  
Fritz Laboratory Report 278.7, October 1963
8. Lay, M. G. and Galambos, T. V.  
THE EXPERIMENTAL BEHAVIOR OF BEAM AND COLUMN SUBASSEMBLAGES  
Fritz Laboratory Report 278.10, 1964
9. WRC-ASCE  
COMMENTARY ON PLASTIC DESIGN Chapter 6: ADDITIONAL  
DESIGN CONSIDERATIONS, ASCE Manual No. 41, 1961
10. Ojalvo, M. and Fukumoto, Y.  
NOMOGRAPHS FOR THE SOLUTION OF BEAM-COLUMN PROBLEMS,  
Welding Research Council Bulletin No. 78, June, 1962

11. Prasad, J. and Galambos, T. V.  
ULTIMATE STRENGTH TABLES FOR BEAM-COLUMNS  
Welding Research Council Bulletin No. 78, June 1962
12. Galambos, T. V.  
INELASTIC LATERAL-TORSIONAL BUCKLING OF WIDE-FLANGE  
BEAM-COLUMNS  
Ph.D. Dissertation, Lehigh University, 1959
13. Ketter, R. L.  
THE INFLUENCE OF RESIDUAL STRESS ON THE STRENGTH  
OF STRUCTURAL MEMBERS  
Proc. of the 7th Technical Session of the Column  
Research Council, 1957
14. Timoshenko, S. P. and Gere, J. M.  
THEORY OF ELASTIC STABILITY  
McGraw Hill, New York, 1961
15. American Institute of Steel Construction  
SPECIFICATION FOR THE DESIGN, FABRICATION AND ERECTION  
OF STRUCTURAL STEEL FOR BUILDINGS  
AISC, New York, 1963
16. CRC  
GUIDE TO DESIGN CRITERIA FOR METAL COMPRESSION MEMBERS  
Column Research Council, Engineering Foundation, 1960
17. Galambos, T. V.  
INELASTIC LATERAL BUCKLING OF BEAMS  
Proc. ASCE, Vol. 89, ST5, October 1963

10. V I T A

The author was born the son of Natale and Antoinette Aglietti on May 4, 1940 at Yonkers, New York. He graduated from Archbishop Stepinac High School in White Plains, New York in June 1958.

The author attended Manhattan College (1958-1962) receiving his Bachelor of Civil Engineering Degree in June 1962. He accepted a research assistantship and worked in the Structural Metals Division at the Fritz Engineering Laboratory at Lehigh University while preparing for the Master of Science Degree in Civil Engineering.